

Characterization of non-metalized SiC detectors using the IBIC technique

C. Torres-Muñoz¹, J. García-López¹, M.C. Jiménez-Ramos¹,
M. Rodríguez-Ramos¹, I. Vila², C. Quintana², G. Pellegrini³

cartormun@alum.us.es

¹ Centro Nacional de Aceleradores (CNA-US-CSIC)

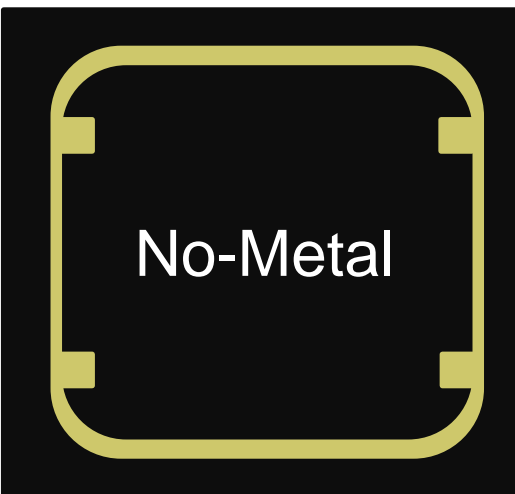
² Instituto de Física de Cantabria (IFCA-UC-CSIC)

³ Instituto de Microelectrónica de Barcelona (IMB-CNM-CSIC)

Context



→ M. C. Jiménez-Ramos *et al.*, 'IBIC analysis of SiC detectors developed for fusion applications', *Radiation Physics and Chemistry*, vol. 177, p. 109100, 2020.



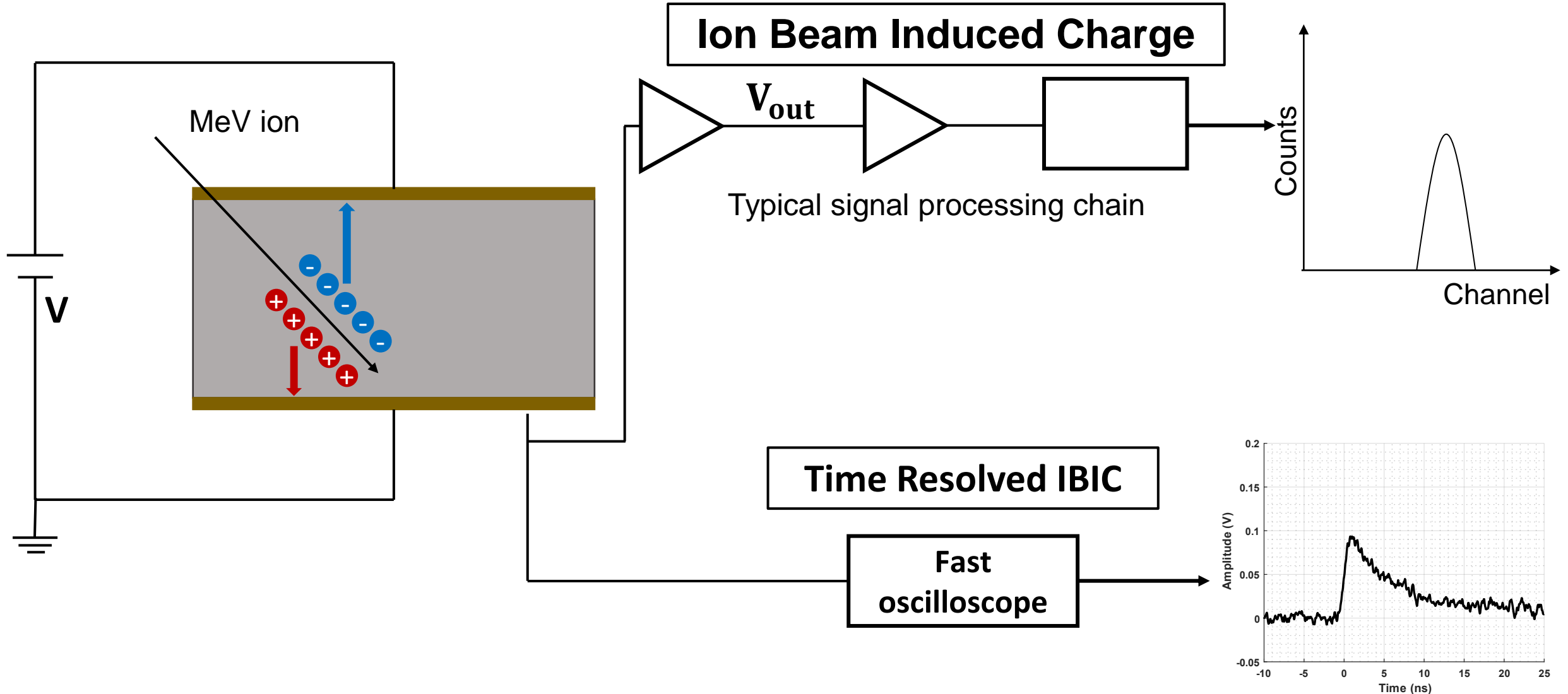
→ E. Currás *et al.*, 'Characterization of neutron irradiated IMB-CNM SiC planar diodes with TPA-TCT', 2022.

- Positional dependence** of the signal profile
- The width of the **sensitive region depends on the fluence**
- Neutron irradiated samples do **not present a diode-like behaviour**



Due to the **unexpected results** obtained with **TPA-TCT (Lasers)**, an experimental campaign was programmed to analyze these results using the **IBIC and TRIBIC techniques (Ion)** at CNA.

IBIC and TRIBIC technique

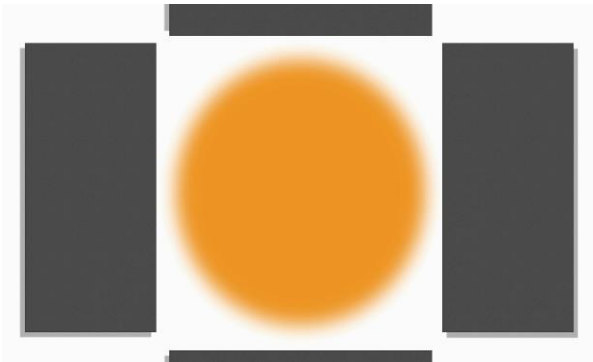


Nuclear microprobe at Tandem3 MV

① RATE

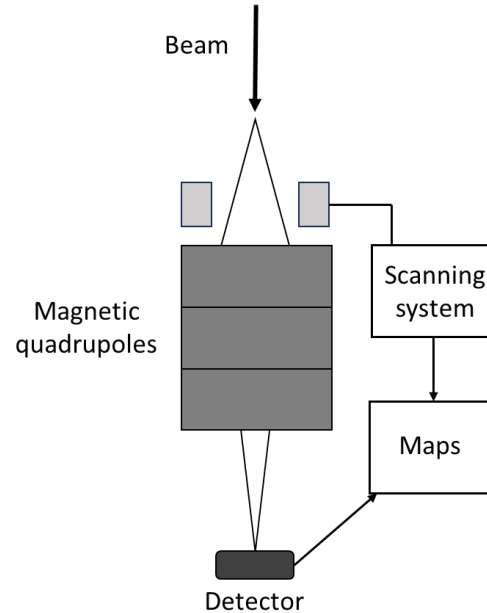
10^{10} p/s

Micrometric slits



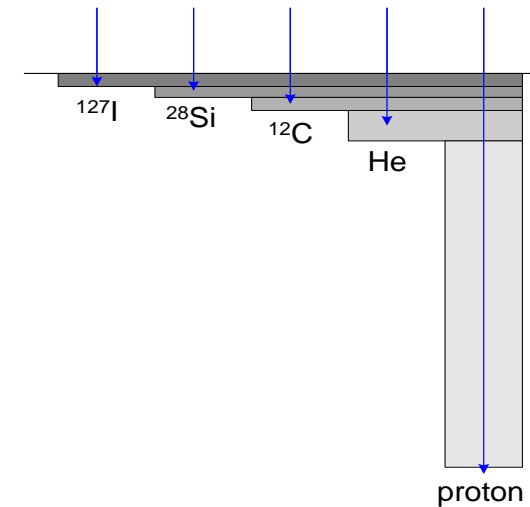
② POSITION

- Focusing and scanning



③ IONS/ENERGIES

- p, α , Li, C, O,..



- ❑ Low count rate: **avoid additional damage (IBIC technique)**

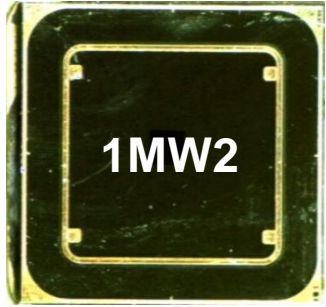
$1 - 10^3$ p/s

- ❑ Scanning system: **few mm²**

- ❑ Synchronous signal acquisition system with scanning: **mappings**

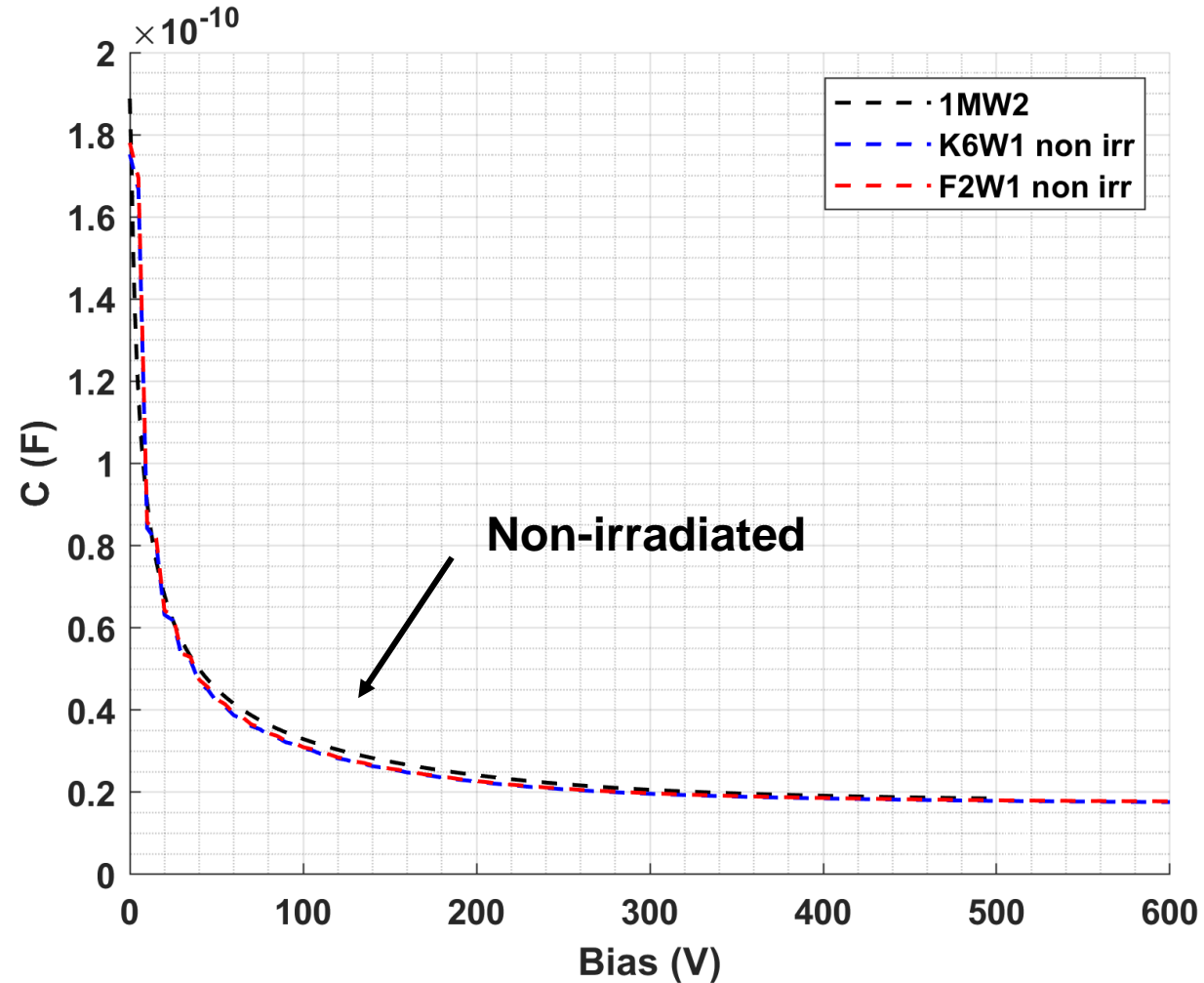
- ❑ Wide range of ions and energies: **explore different depths**

Neutron irradiated detectors do not present a diode-like behaviour

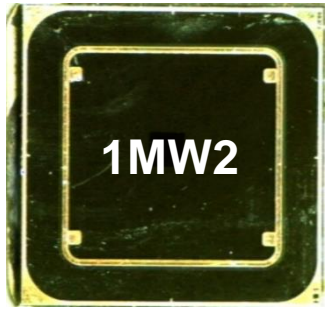


Pristine

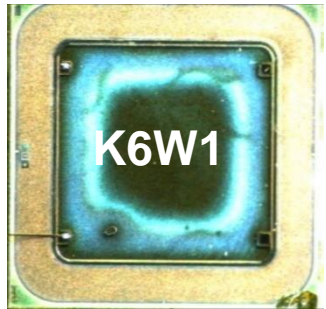
Non-metallized SiC detector with a passivation layer



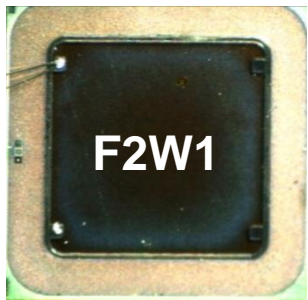
Neutron irradiated detectors do not present a diode-like behaviour



Pristine

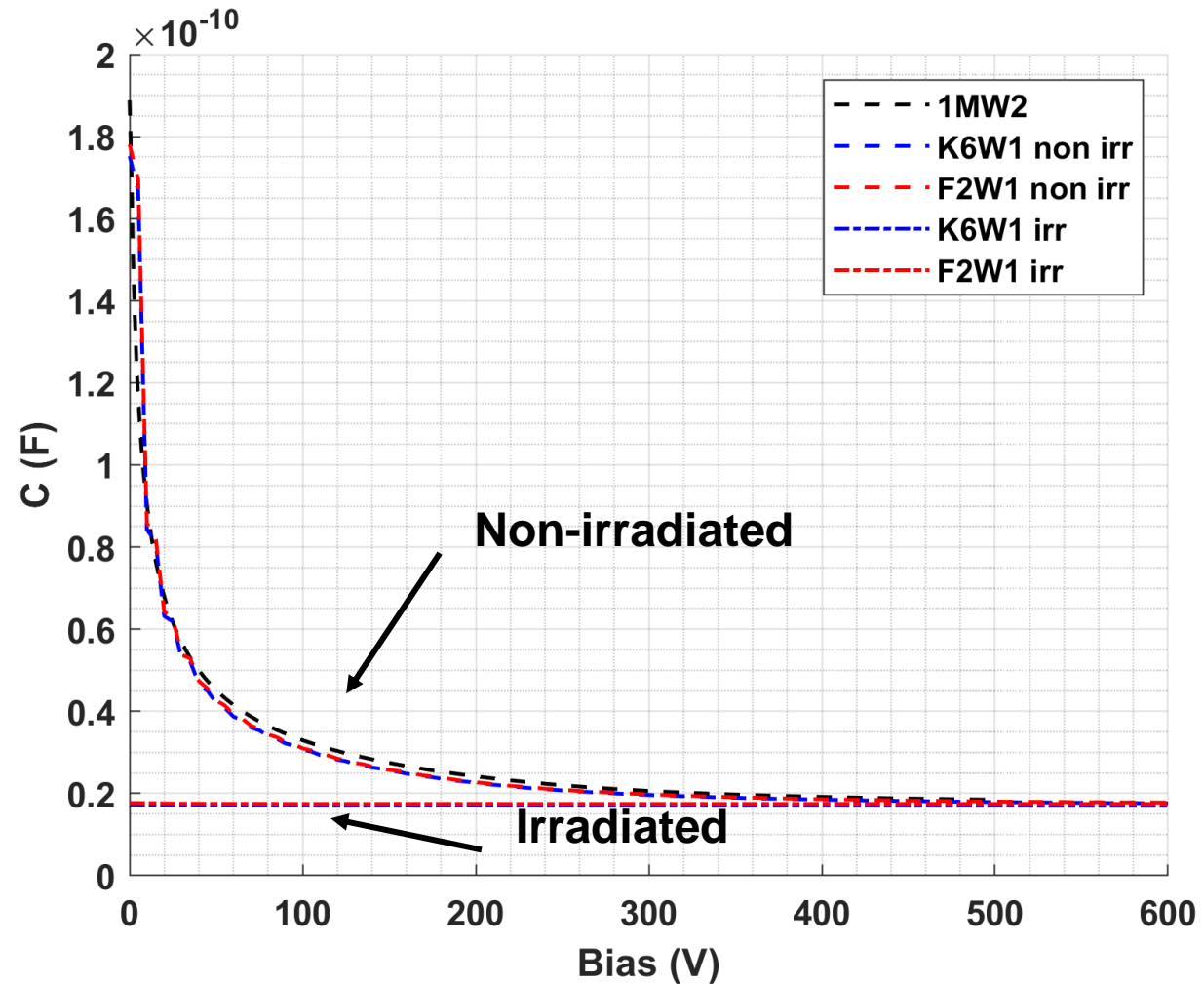


$4 \times 10^{14} n_{eq}/cm^2$

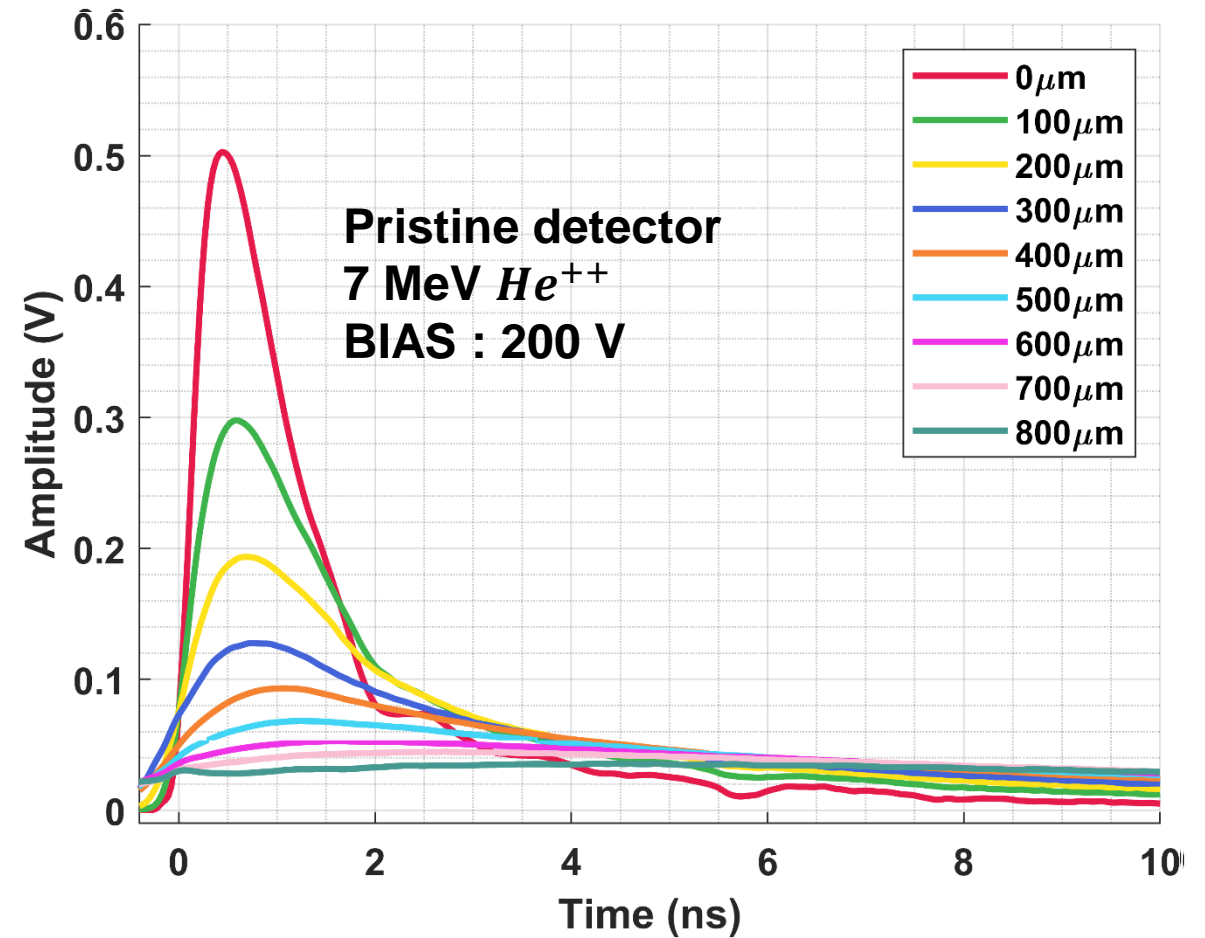
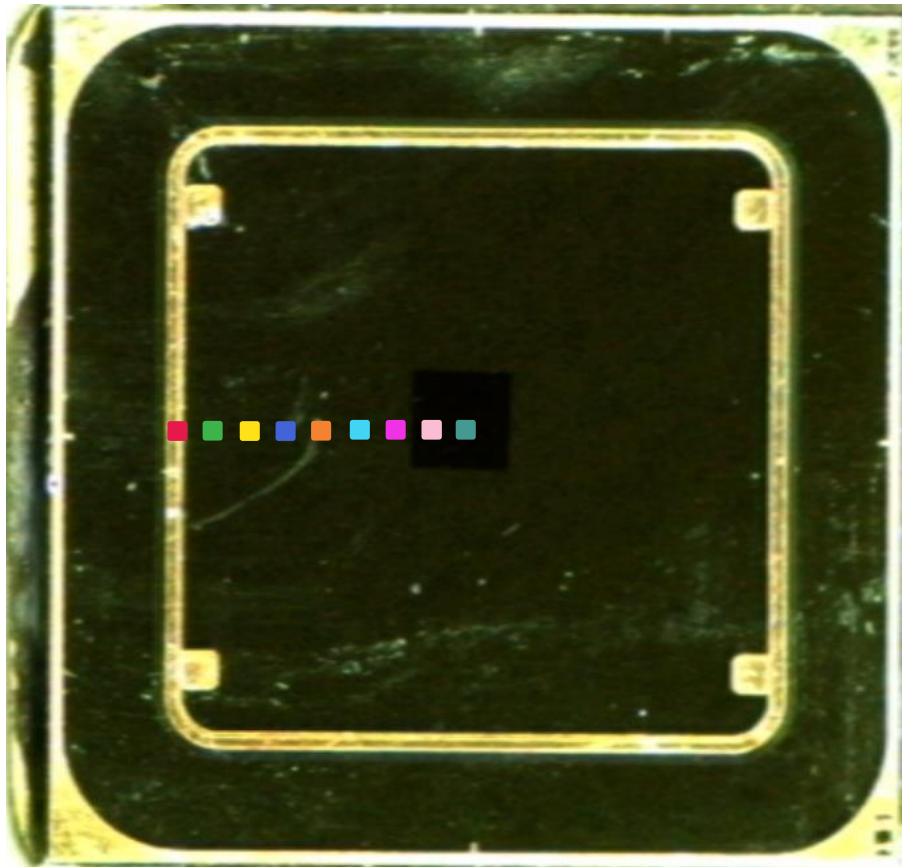


$1 \times 10^{15} n_{eq}/cm^2$

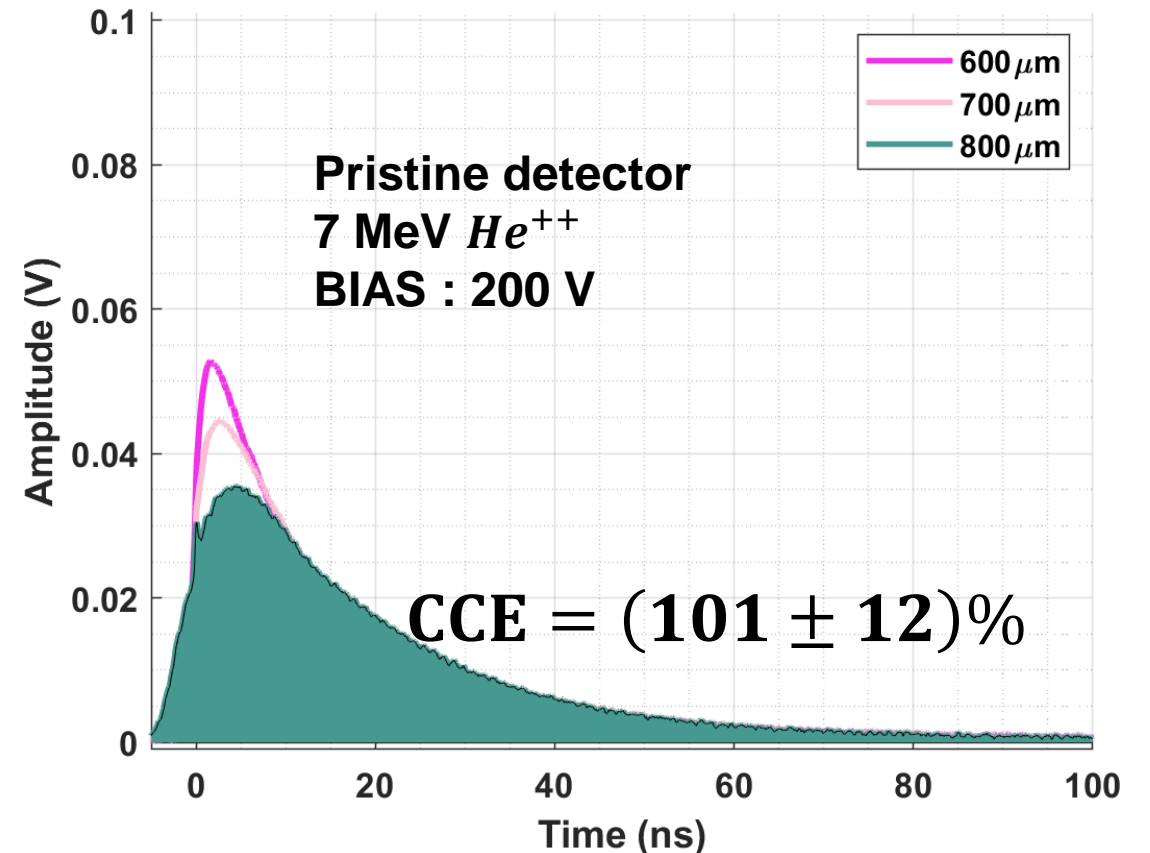
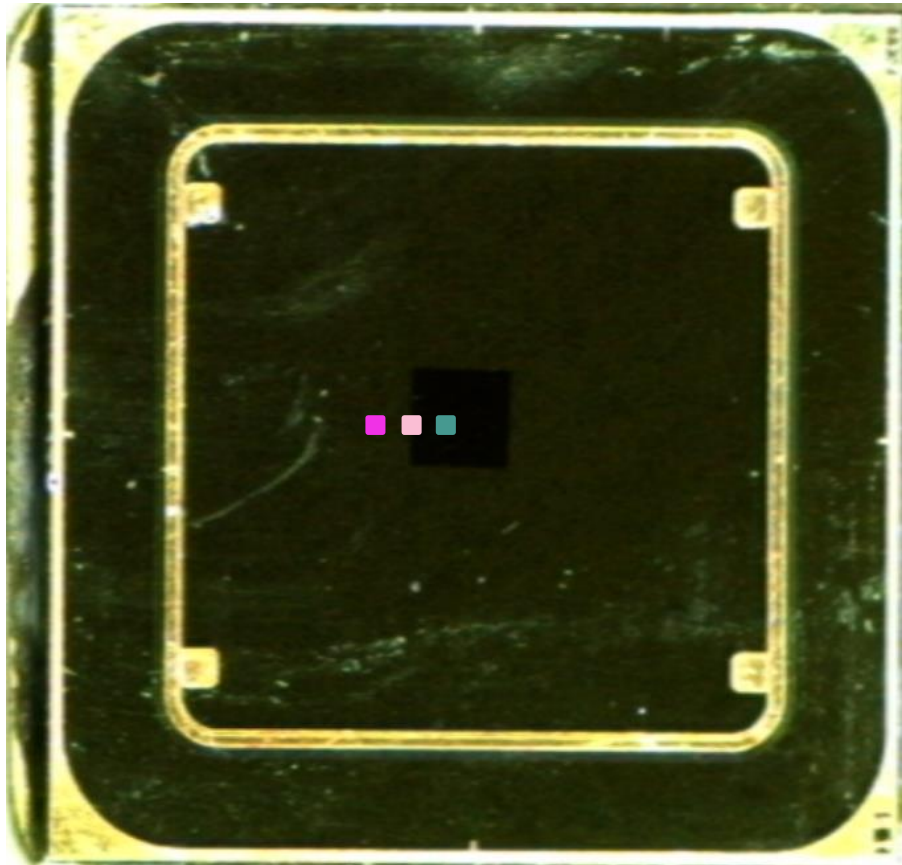
Non-metallized SiC detector with a passivation layer



Waveform depends on position



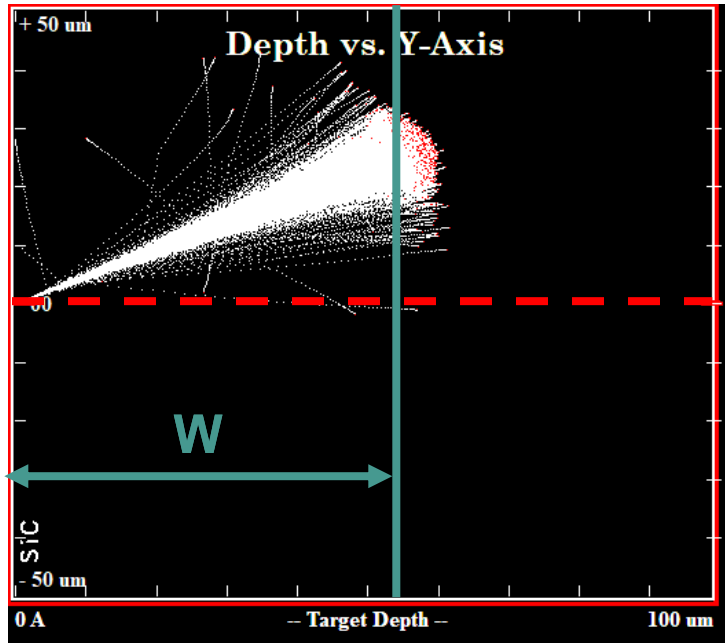
Detector with 100% of CCE



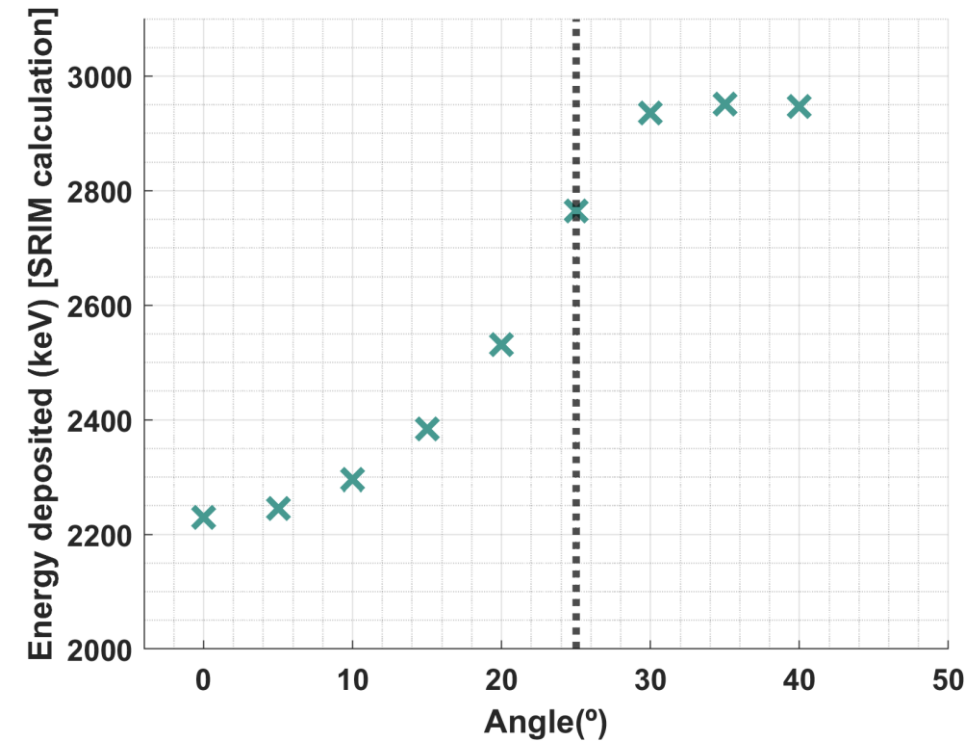
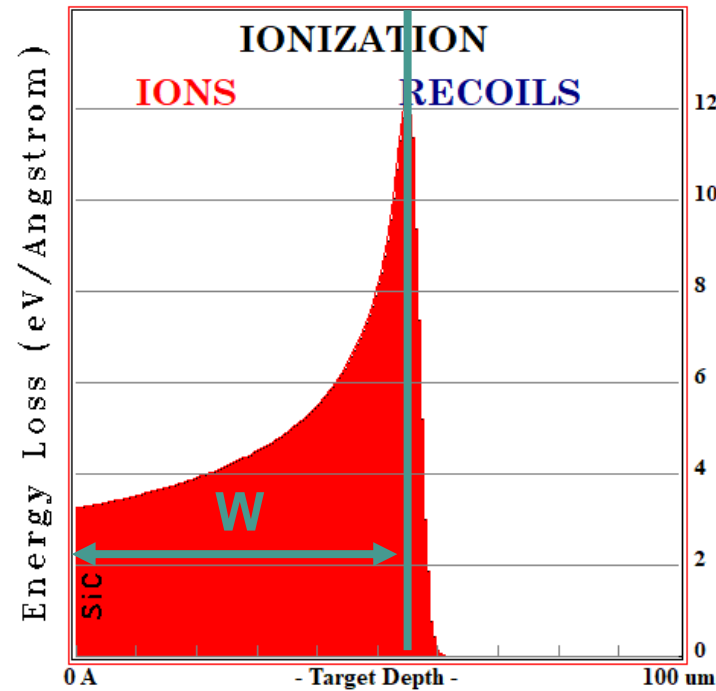
Charge Collection Efficiency (CCE)

$$CCE = \frac{\text{Charge induced}}{\text{Charge generated}}$$

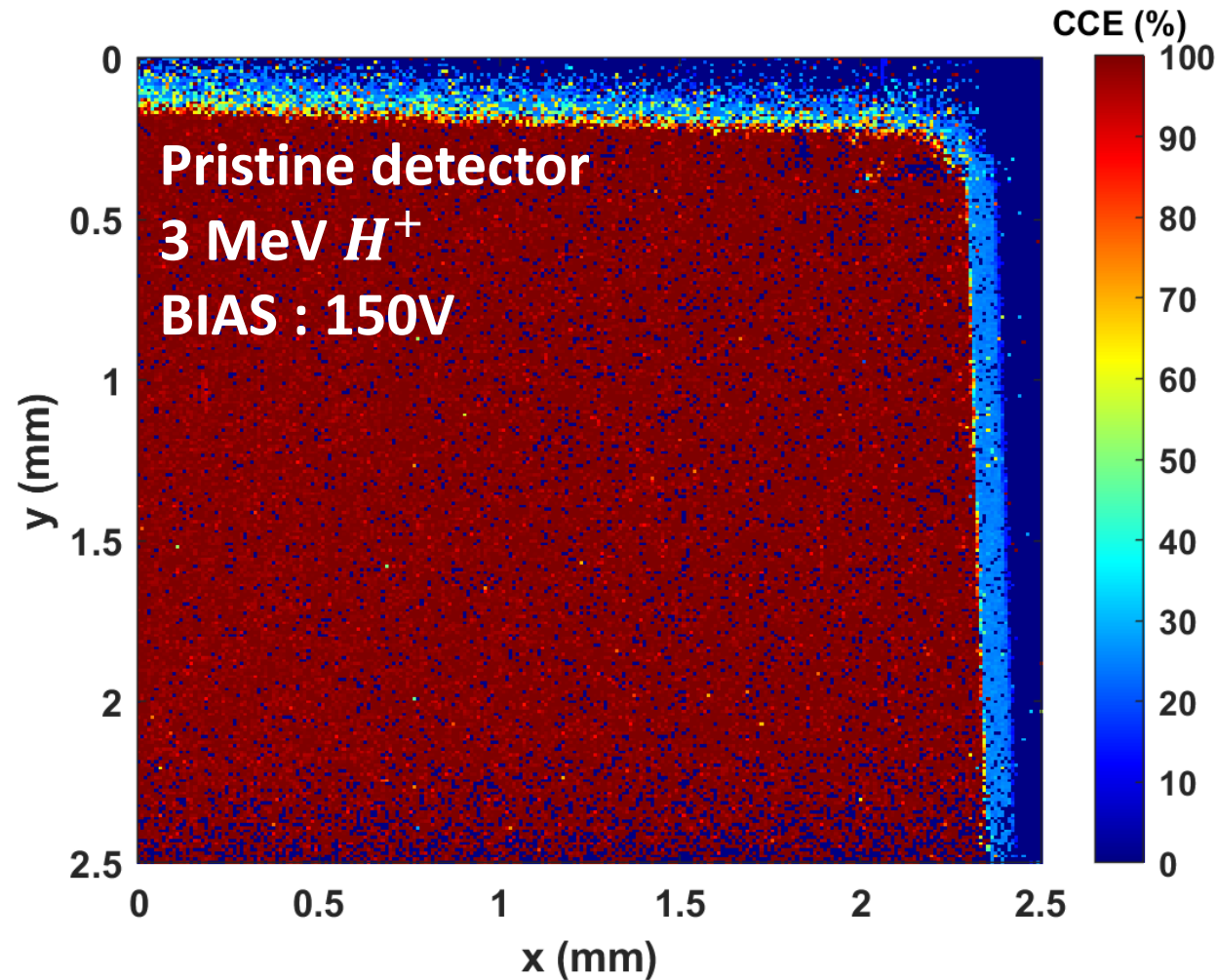
Methodology to calculate depletion zone



$$E_{dep}(W, \theta) = \int_0^W \frac{dE}{dx}(\theta) dx$$



CCE homogeneity



IBIC Map. Scan size: $2.5 \times 2.5 \text{ mm}^2$

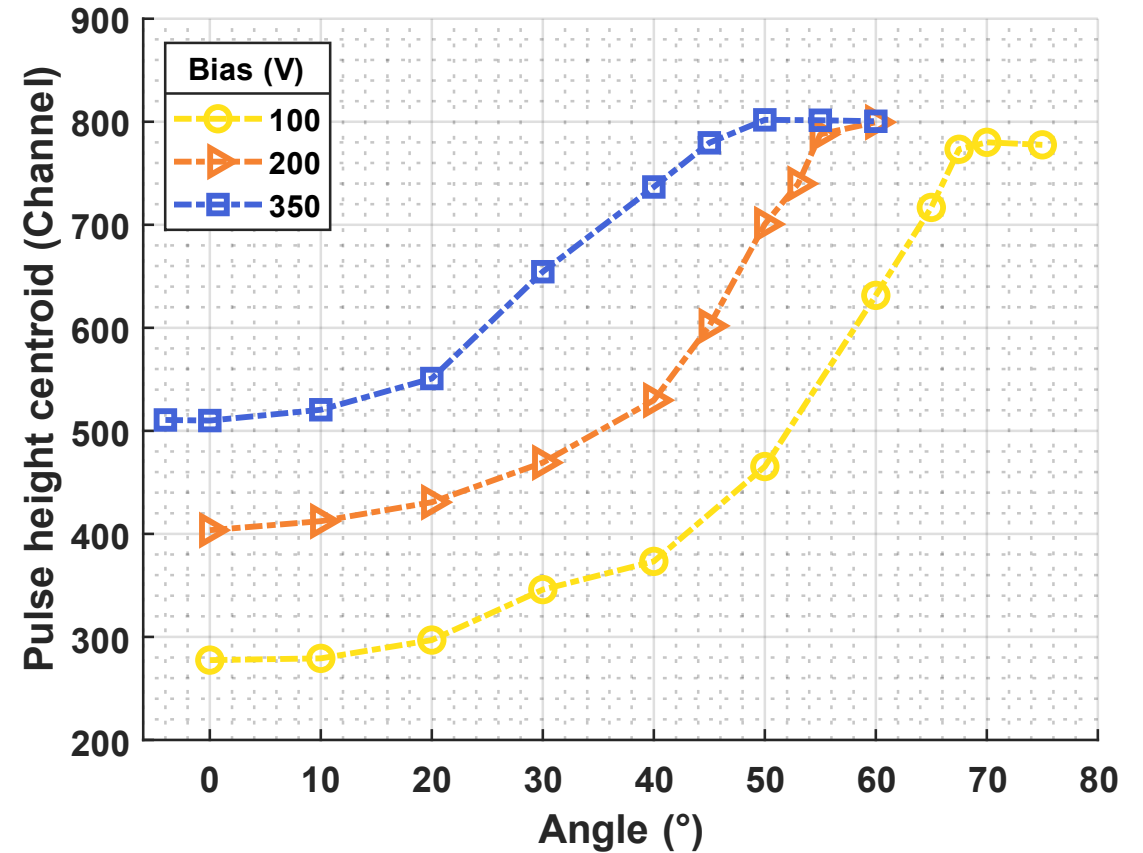
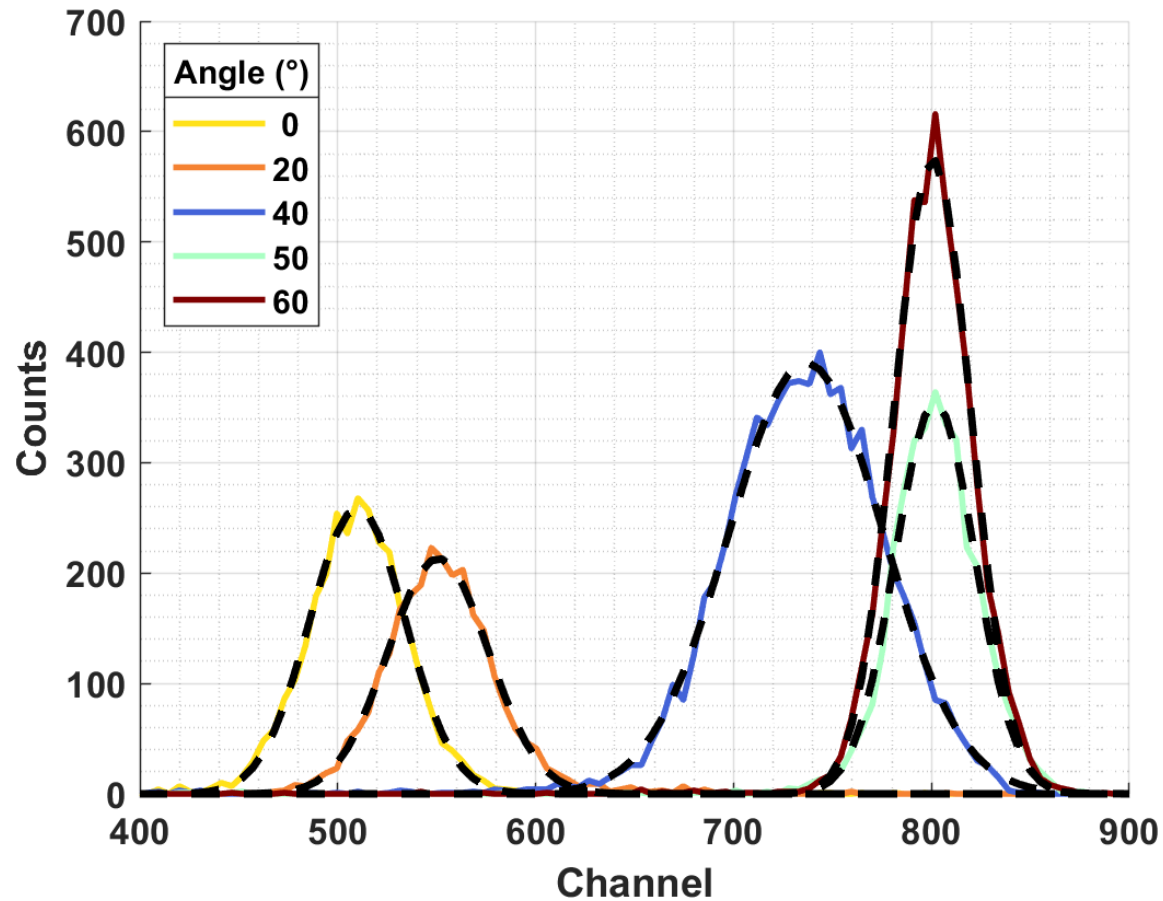
Even though position-
dependence of
waveform



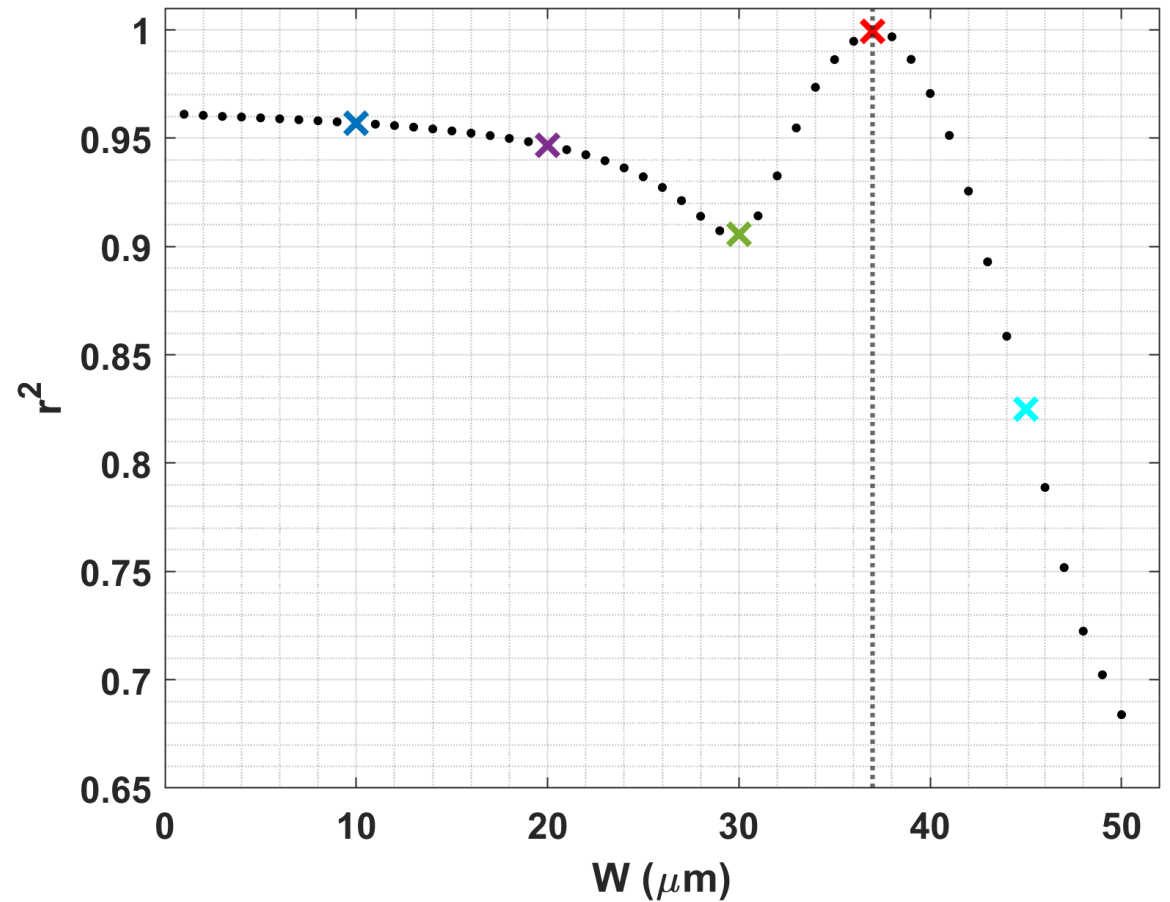
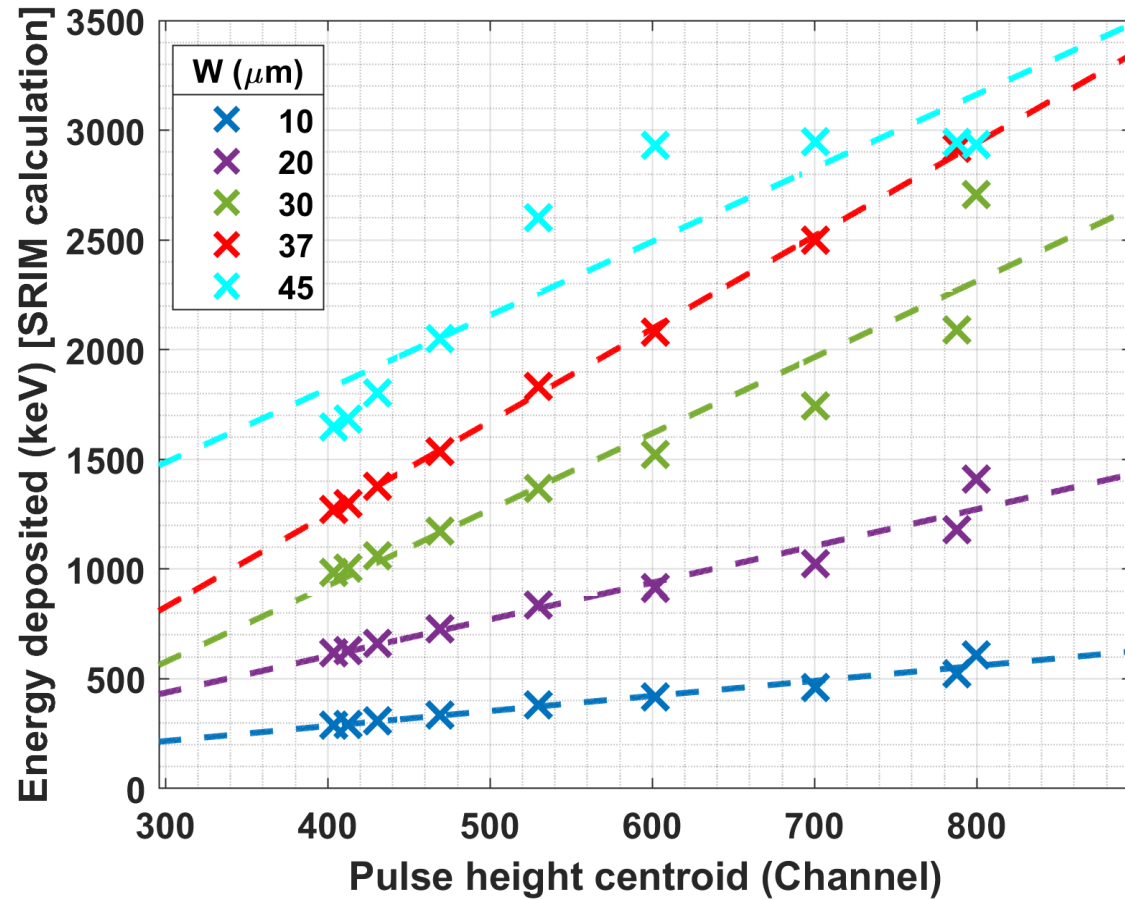
CCE is not
radial position
dependent

Pristine detector experimental curves

Pristine detector. Protons 3 MeV. Bias = 350 V

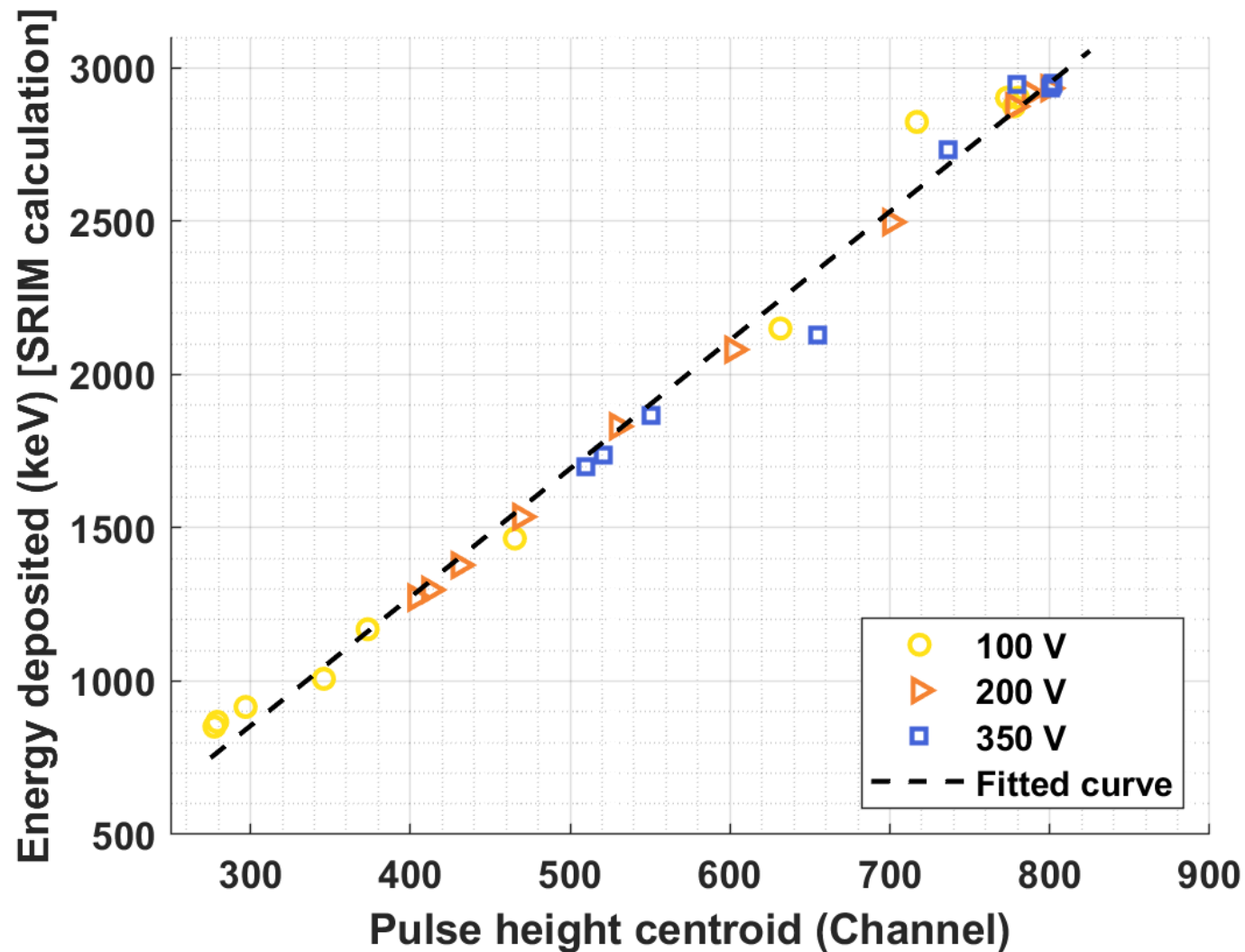


Calibration calculation using SRIM



Pristine detector. Protons 3 MeV. Bias = 200 V

Calibration energy-channel

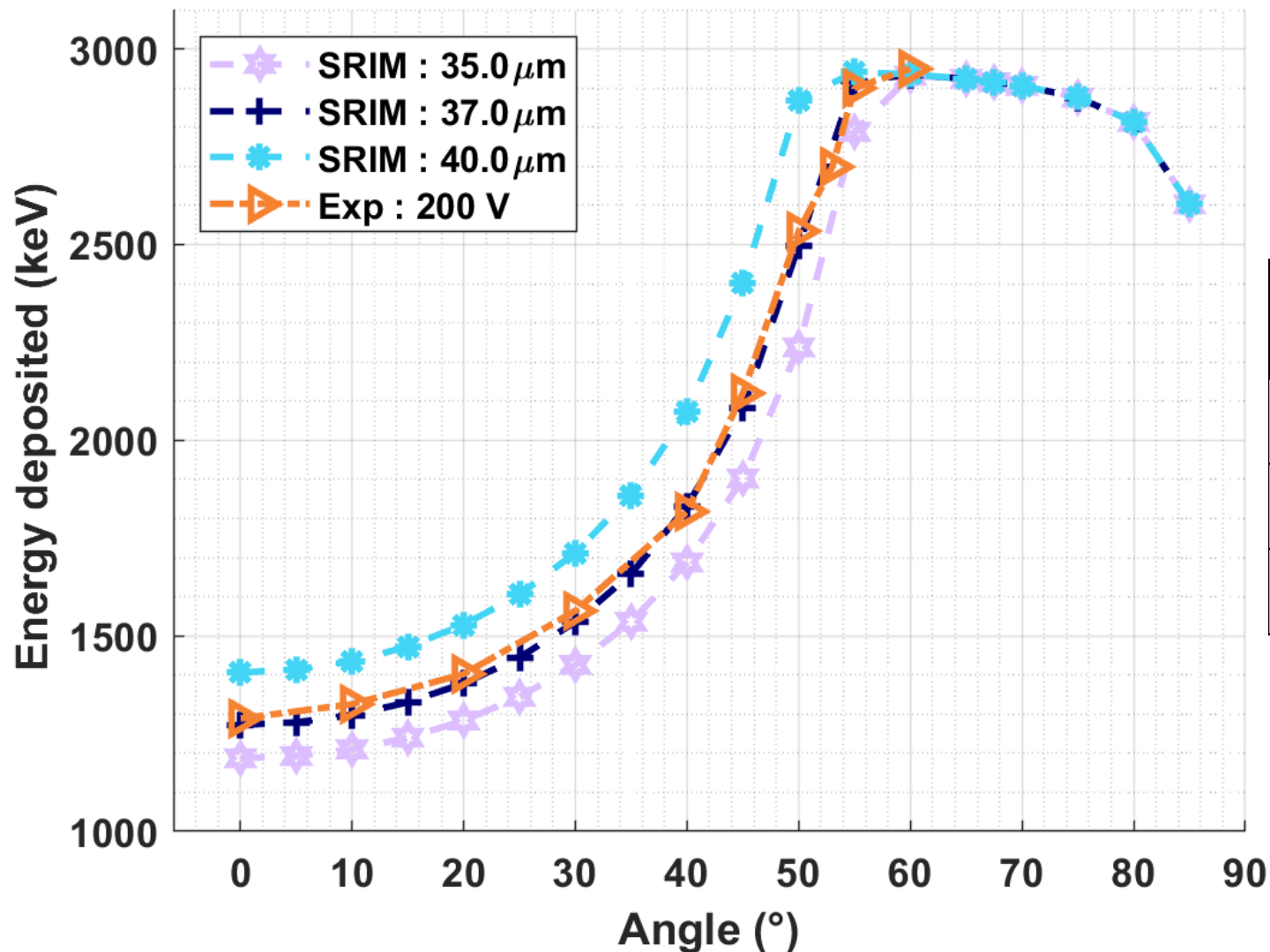


Pristine detector. Protons 3 MeV.

- Detector with 100% of CCE (TRIBIC)
- Theoretical deposited energy (SRIM) for each W and rotation angle
- Calibration with all experimental data
- The obtained W corresponds to the line with the best r^2

Agreement of experimental and simulated curves

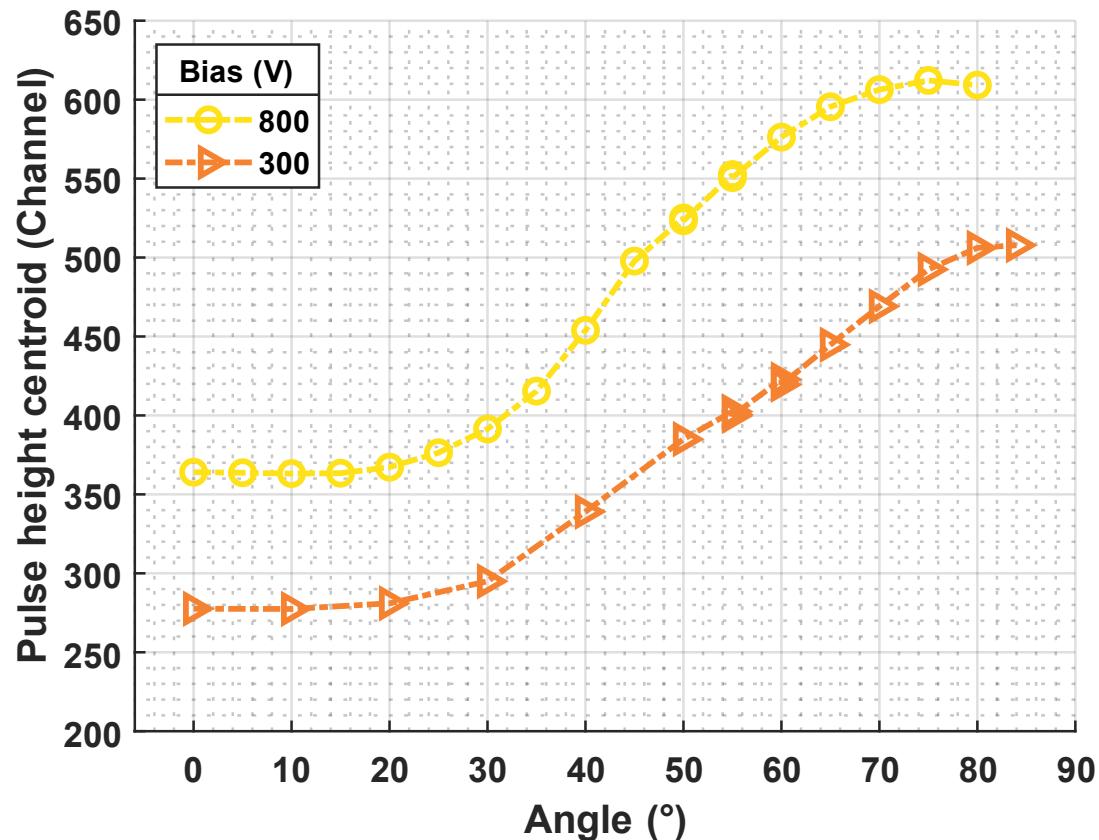
Pristine detector. Protons 3 MeV. Bias = 200 V



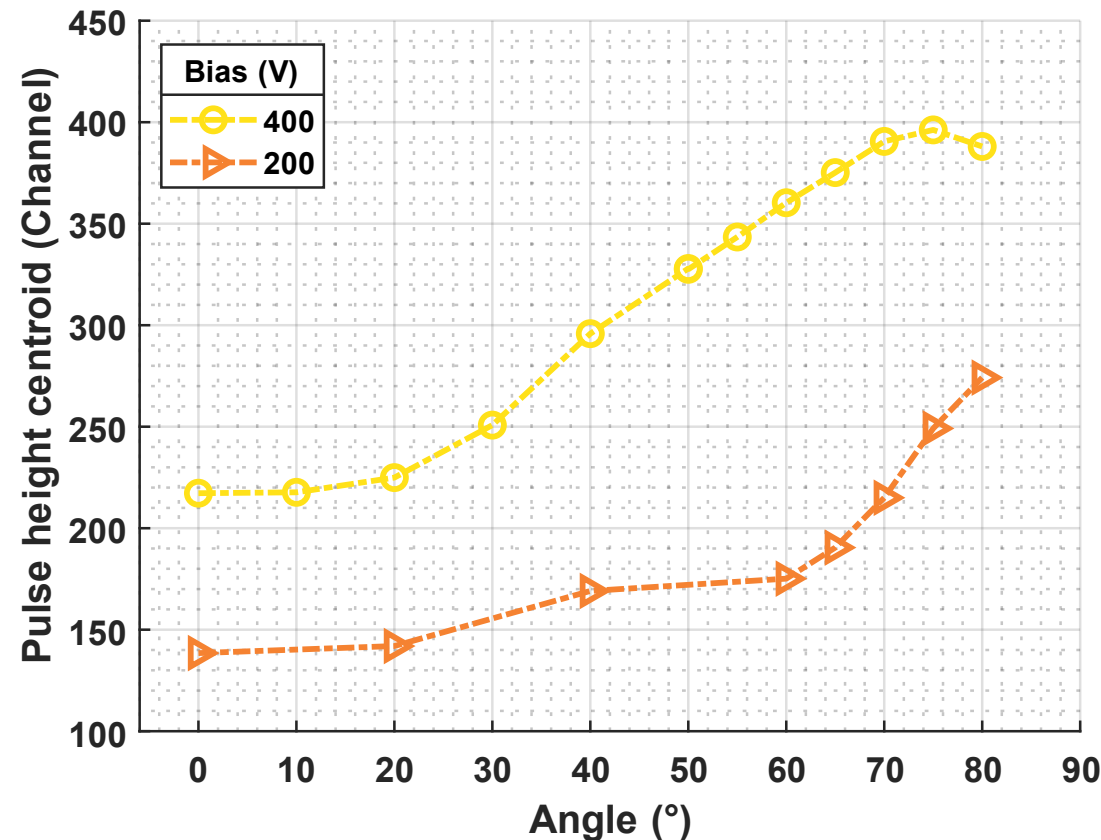
Bias (V)	(W-IBIC ± 1) (μm)	W-TPA (μm)	W- CV (μm)
350	46	43	39
200	37	36	32
100	27	27	23

Irradiated detectors experimental curves

K6W1 ($4 \times 10^{14} n_{eq}/cm^2$)



F2W1 ($1 \times 10^{15} n_{eq}/cm^2$)



Calculated depletion zone

Detector	Bias (V)	(W-IBIC \pm 1) (μ m)	W-TPA (μ m)	W-CV (μ m)
Pristine	350	46	43	39
	200	37	36	32
	100	27	27	23
$4 \times 10^{14} n_{eq}/cm^2$	800	20-25	25	45
	300	15-20	20	46
$1 \times 10^{15} n_{eq}/cm^2$	400	20-25	20	44
	200	15-20	17	44

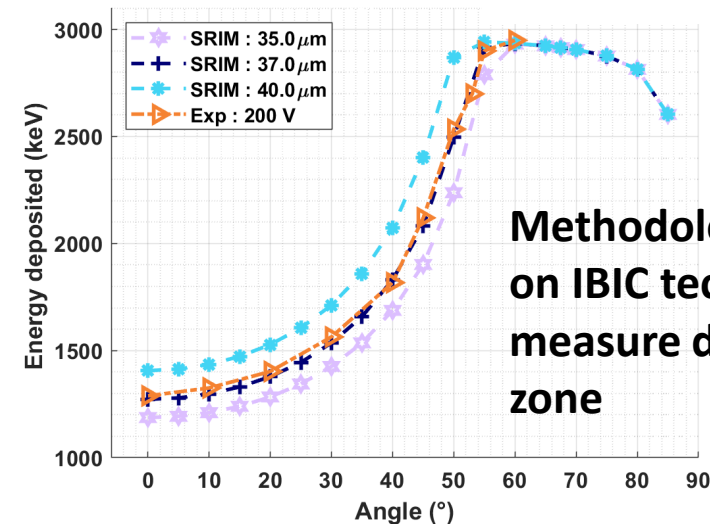
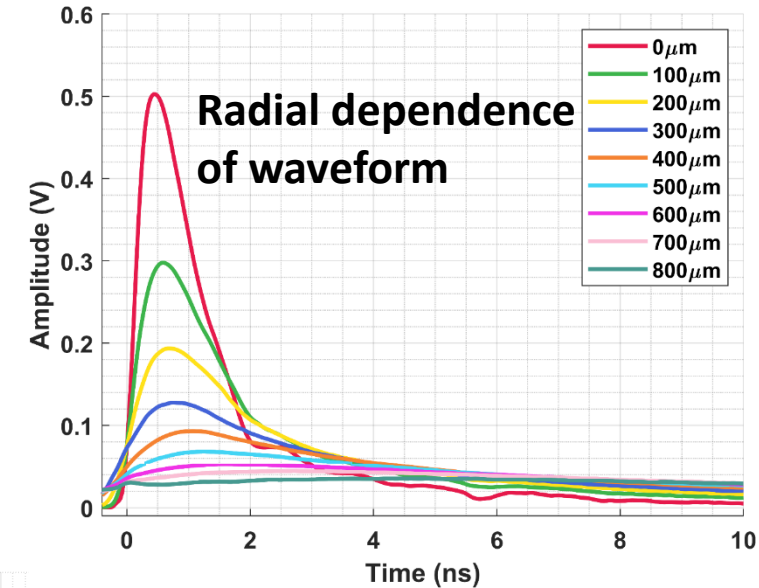
☐ Results in agreement with TPA-TCT results

☐ The size of the depletion zone decreases with neutron fluence.

☐ Variation with voltage in irradiated detectors is small

Conclusions

- ❑ Methodology based on IBIC technique to measure depletion zone
- ❑ Radial dependence of waveform: Signals varied with radial position, with signals at the edges being faster and those in the center slower.
- ❑ The results obtained with the TRIBIC and IBIC techniques are compatible and confirm the results obtained with the TPA-TCT technique.



Thanks for your attention!

M.C. Jiménez-Ramos acknowledges the support to this work
through a VI PPIT-US contract

Back-up

Why Silicon Carbide radiation detectors ?

Property	4H-SiC	Si
E_g at (300 K)[eV]	3.23	1.12
ρ [g/cm ³]	3.22	2.33
μ_e [cm ² /V · s]	800	1450
μ_h [cm ² /V · s]	115	450
Thermal conductivity [W/m · K]	490	130
$E_{breakdown}$ [MV/cm]	3 – 4	2.2
Atomic displacement threshold [eV]	22 – 35	13 – 20
$e^- - h^+$ energy [eV]	7.28	3.6
v_{sat} [10 ⁷ cm/s]	2	0.8

Wide bandgap :

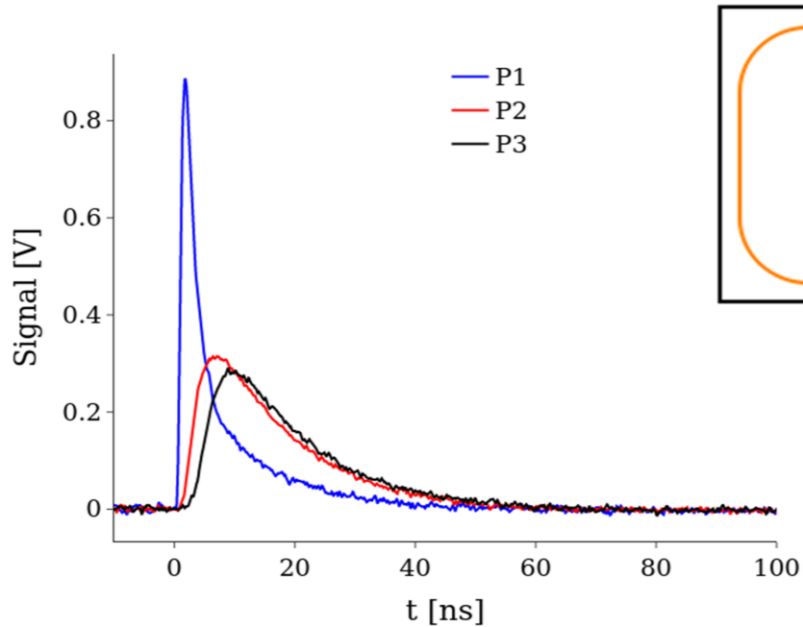
- Reduces the leakage current and noise level
- Visible blind

Higher Breakdown and higher displacement threshold :

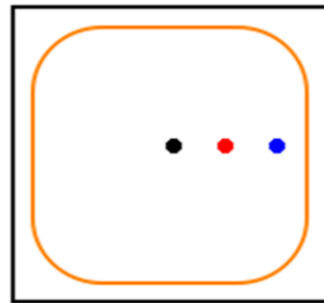
- Advantage for Radiations hardness

TPA-TCT results

1MW2 - Transient currents



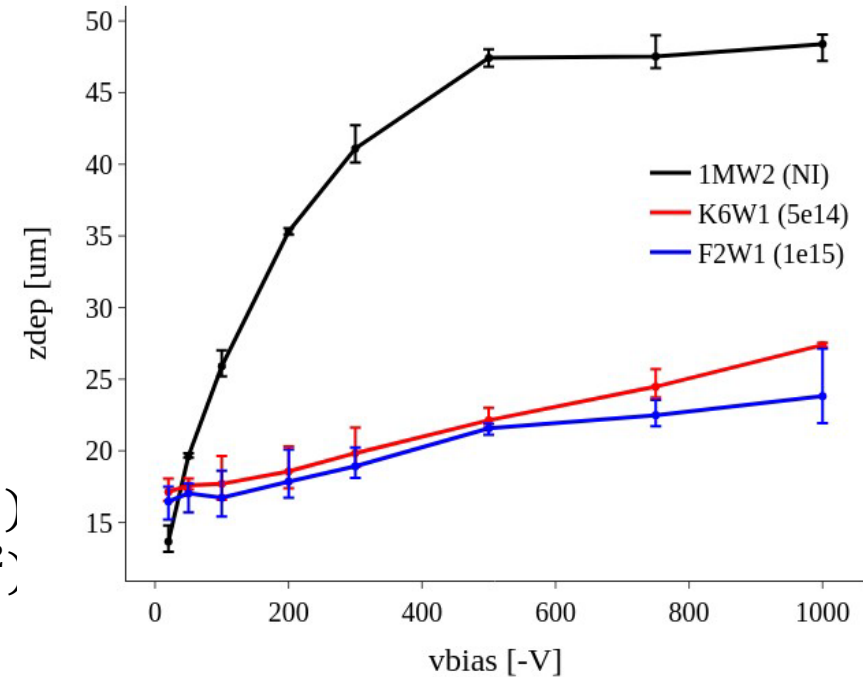
1MW2 Scheme:



Samples (**non metallized contact**):

- 1MW2 (Non-irradiated)
- F2W1 ($1 \times 10^{15} n_{eq}/cm^2$)
- K6W1 ($4 \times 10^{14} n_{eq}/cm^2$)

Depletion width bias dependence

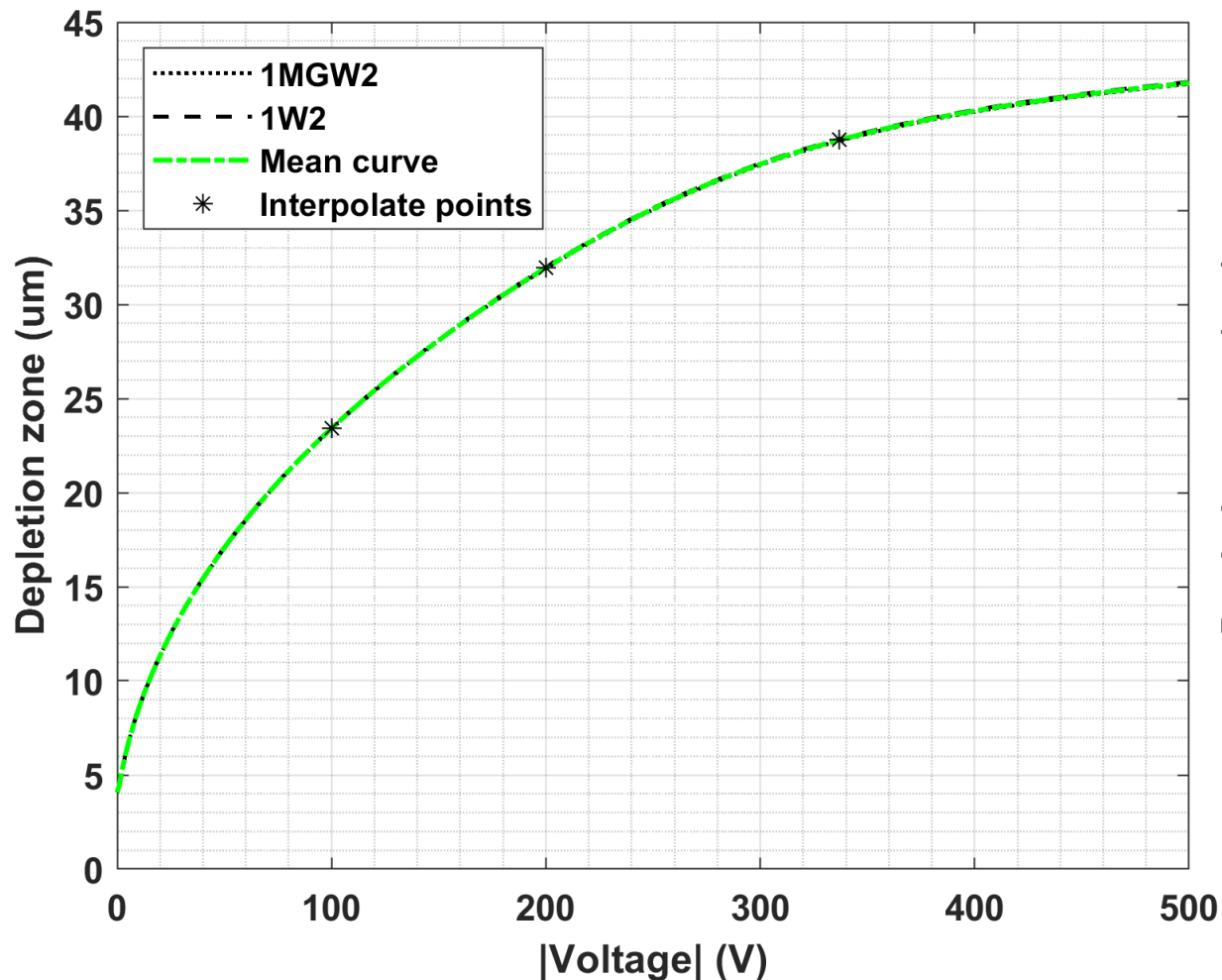


“Characterization of neutron irradiated IMB-CNM SiC planar diodes with **TPA-TCT**”:

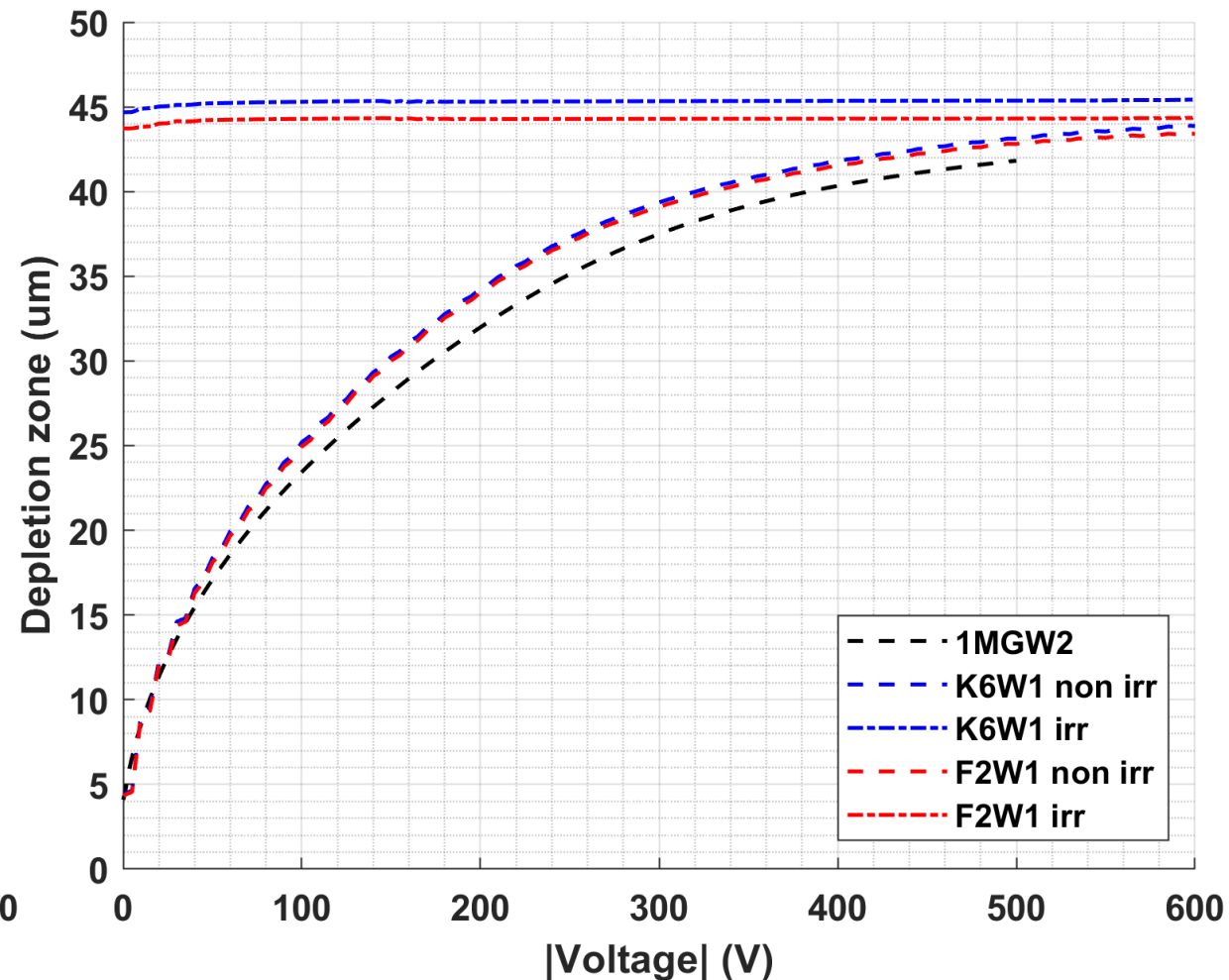
- Positional dependence of the signal profile
- The width of the sensitive region depends on the fluence

Electric measurements

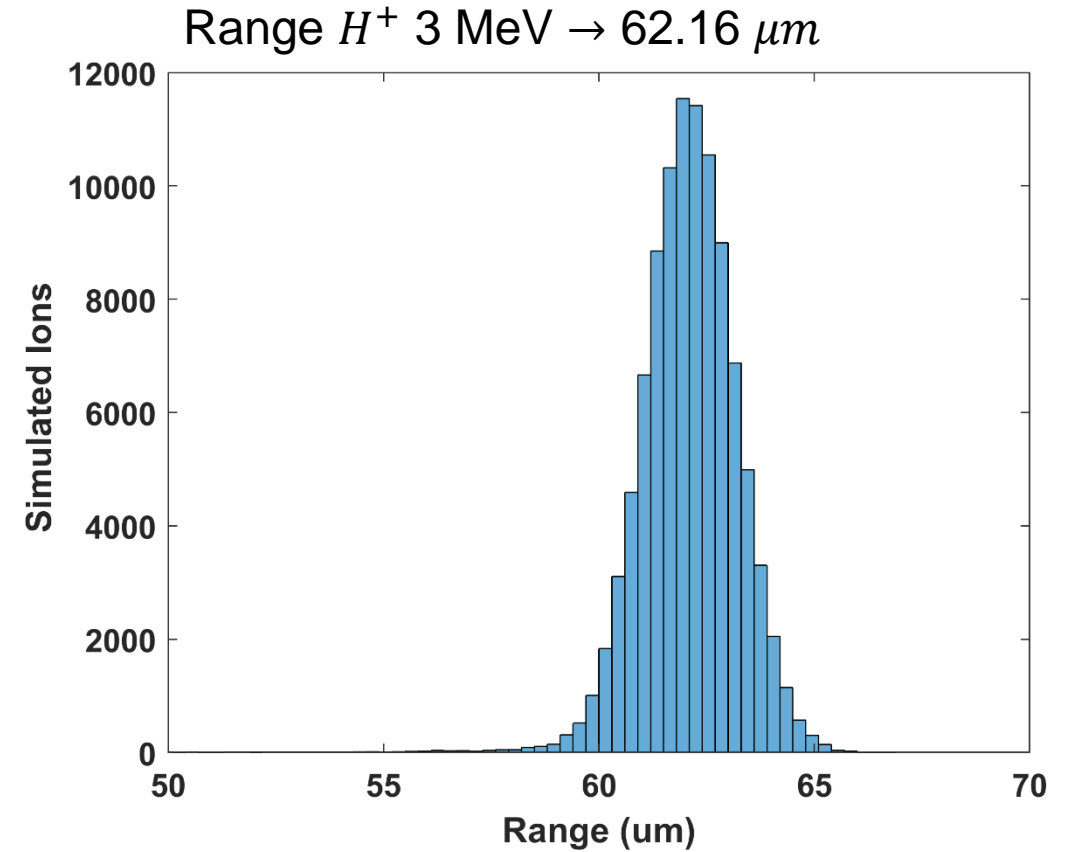
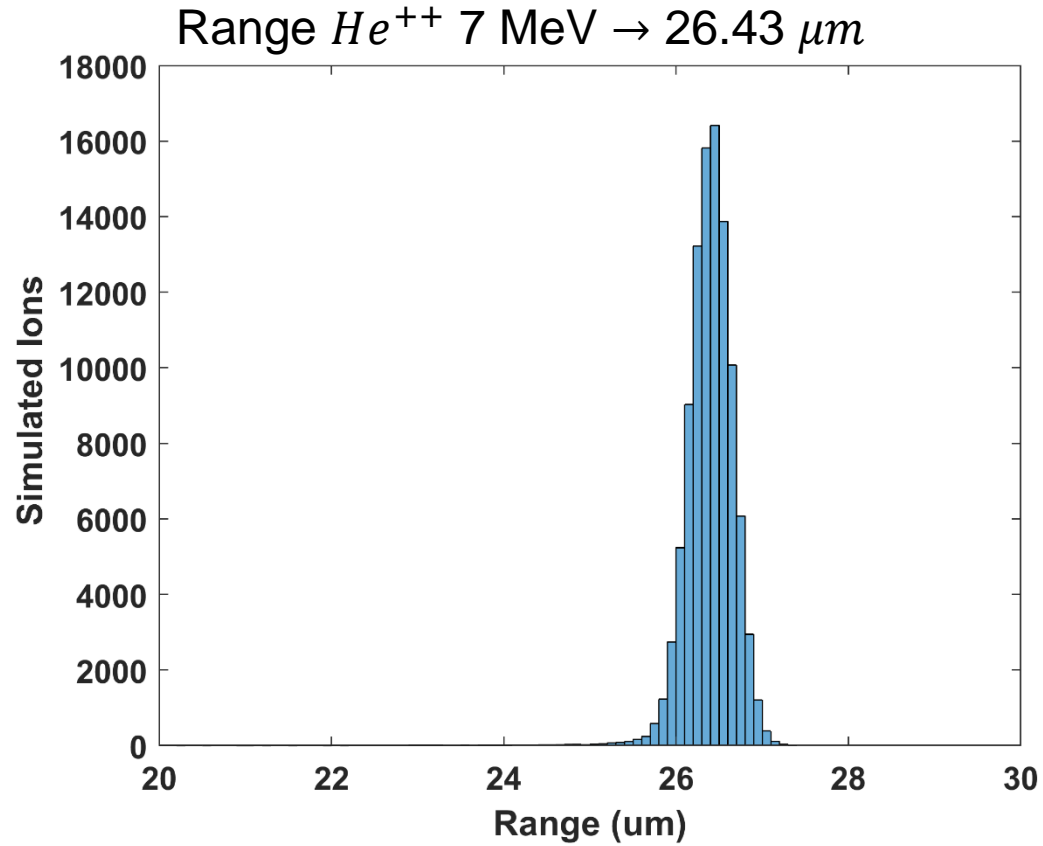
Pristine detector



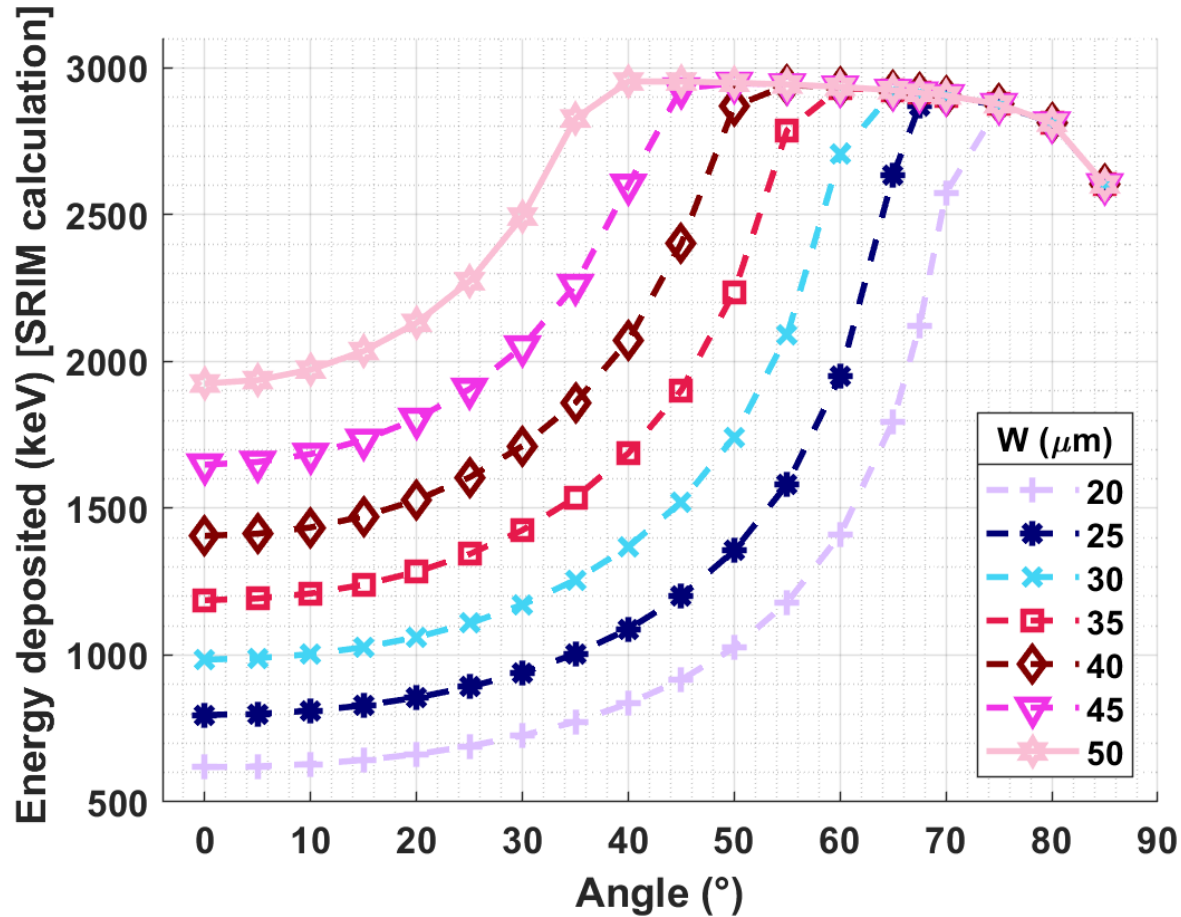
Irradiated detectors



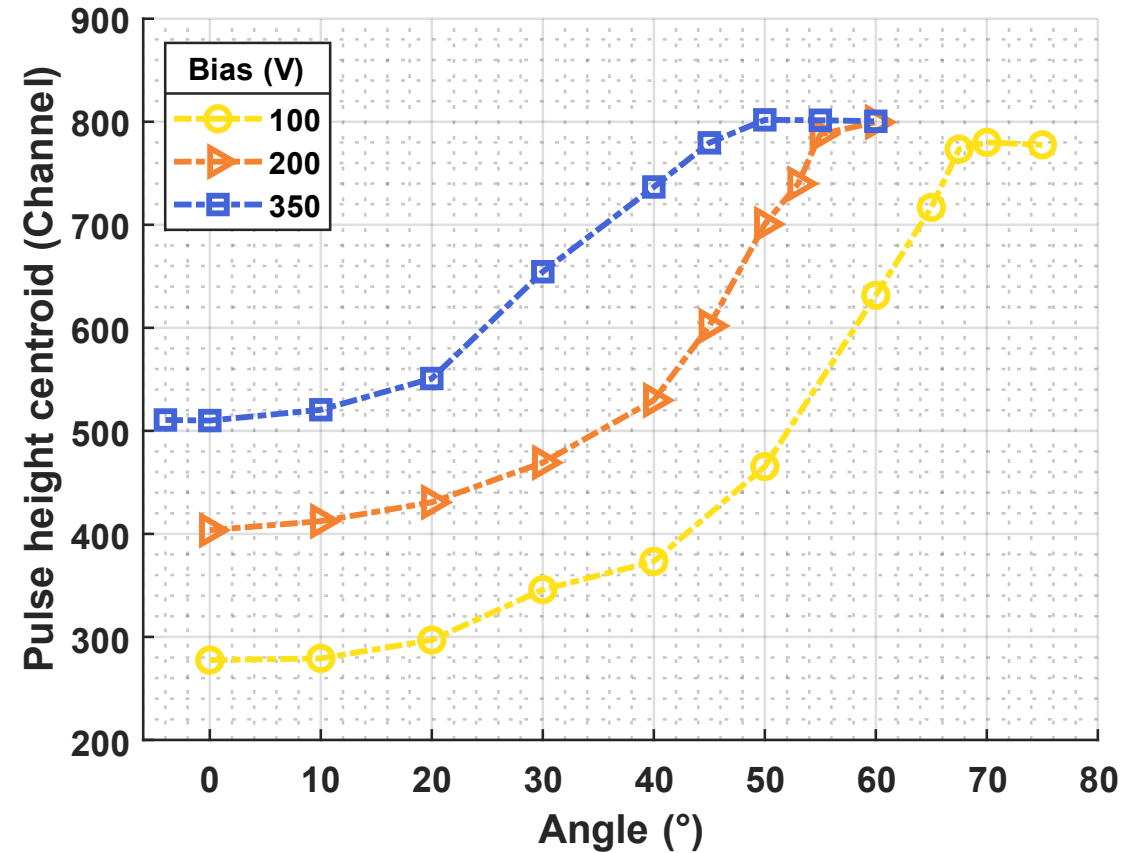
SRIM Simulation (Range on SiC)



Simulations and experimental results

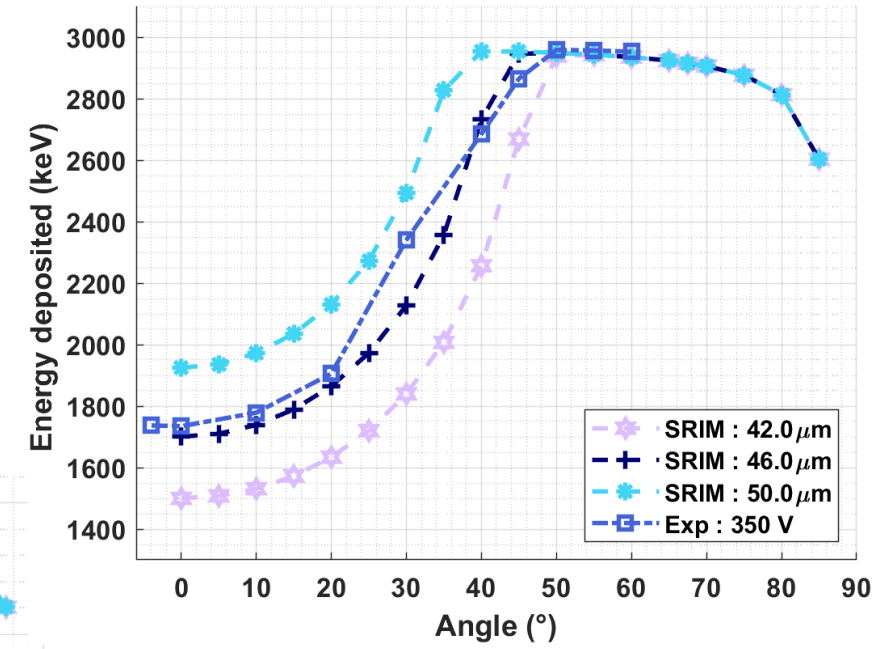
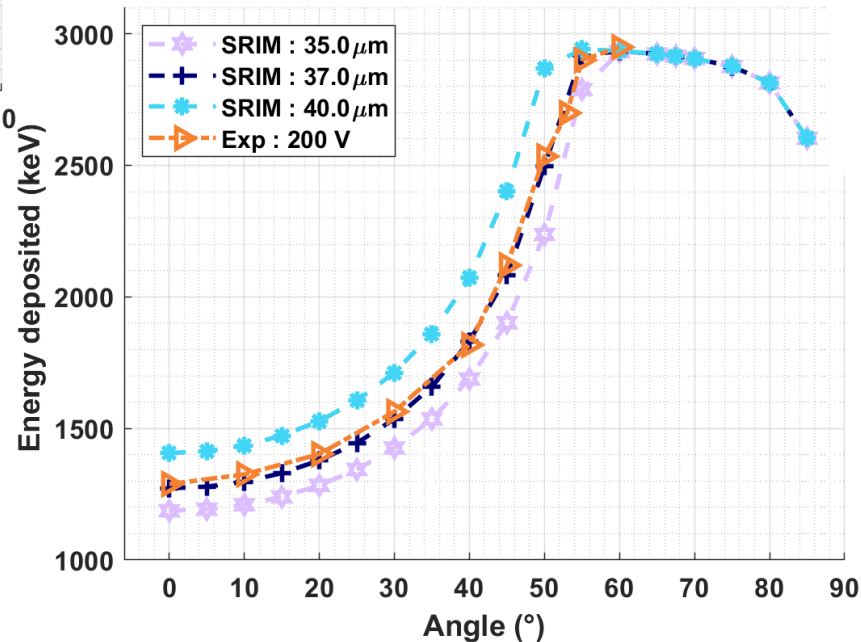
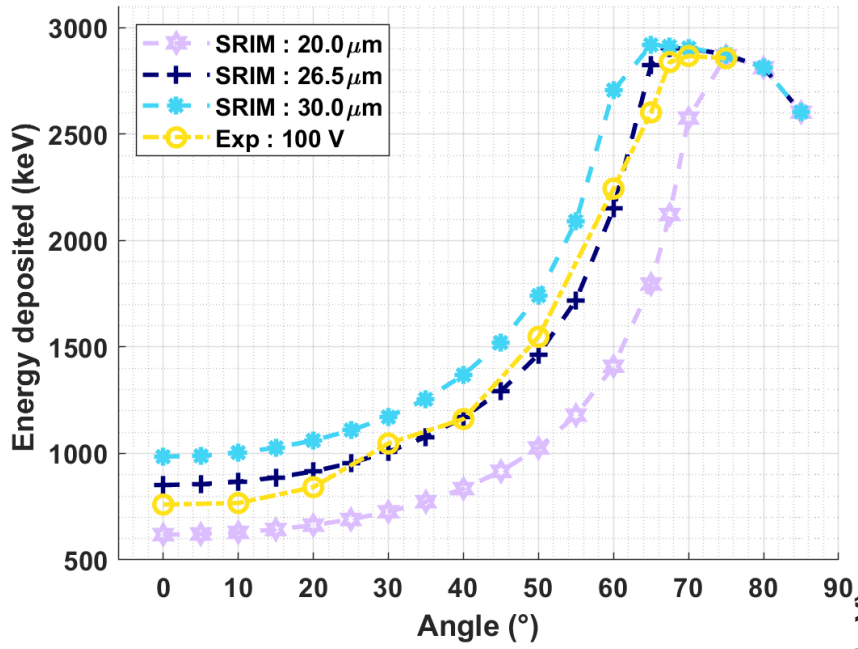


Simulated curves obtained with SRIM

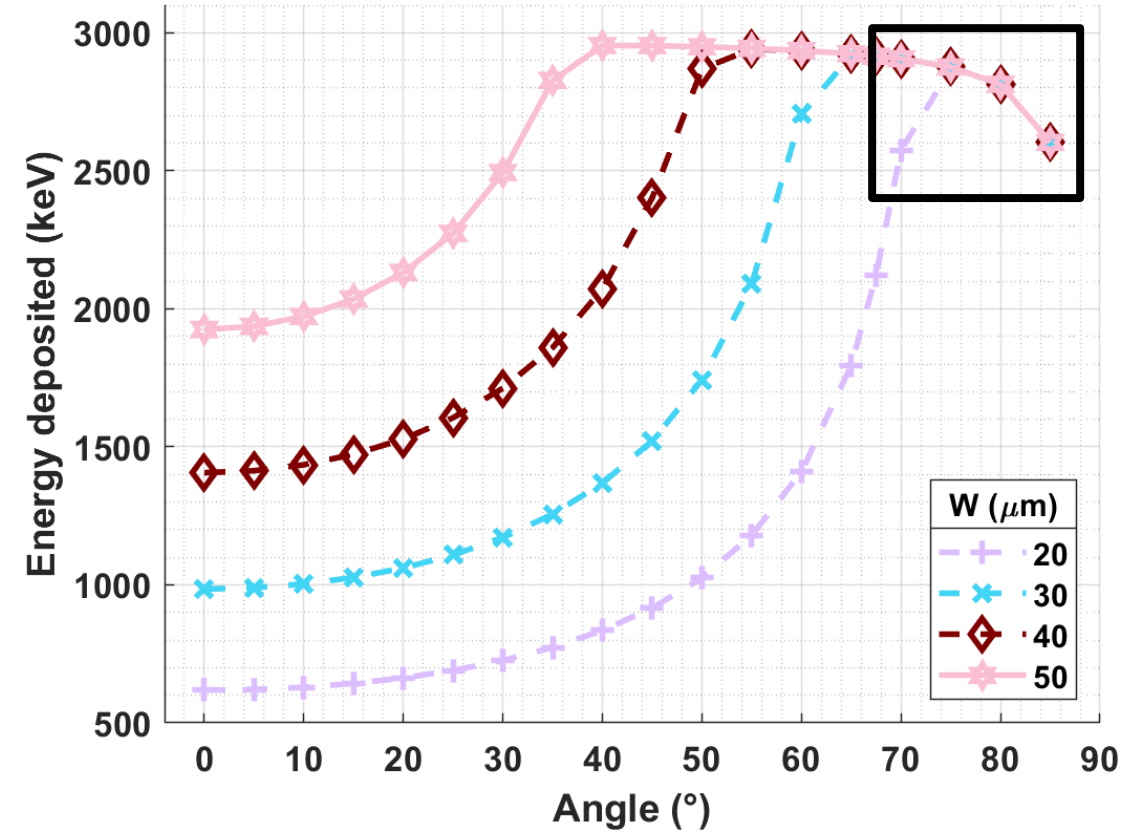
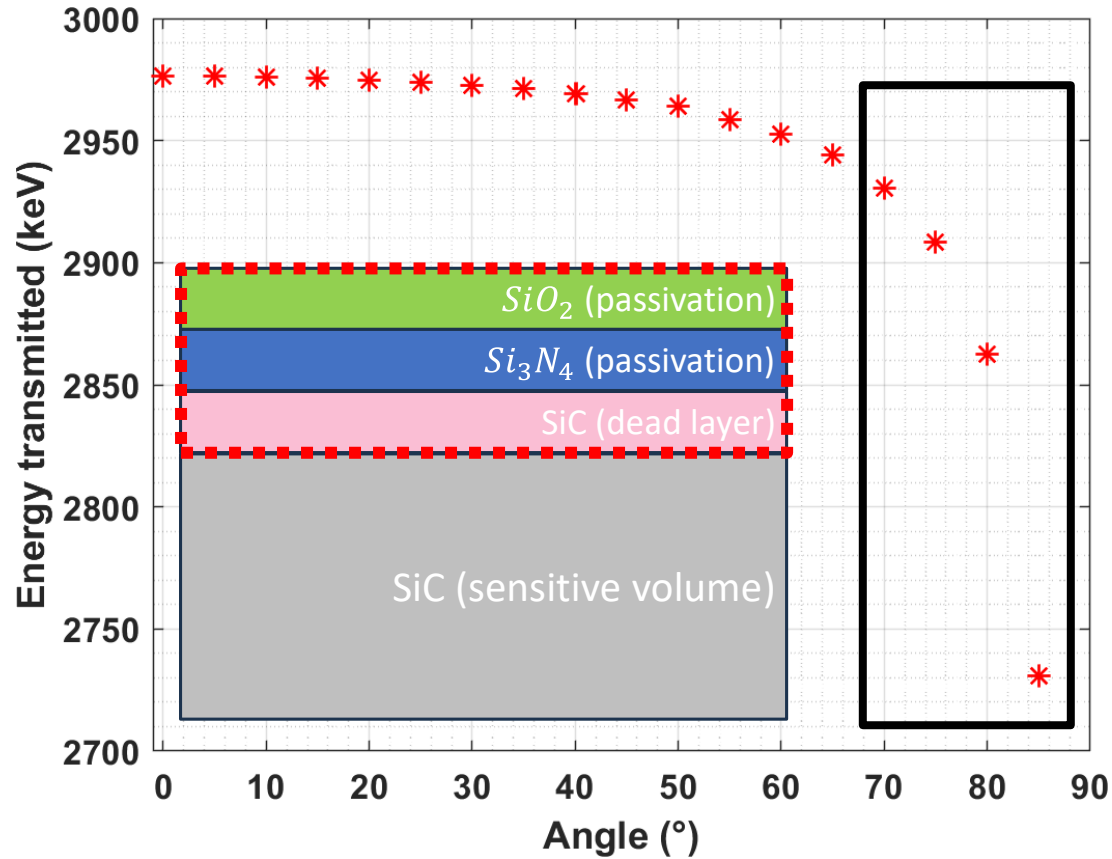


Experimental results (Pristine detector)

Calibrated experimental curves



SRIM simulations (3 MeV H⁺)



Calculation of the absolute CCE value for the pristine detector

Theoretical calculation :

- Deposited energy in detector [SRIM simulation] : $E = (6861 \pm 22) \text{ keV}$
- Electron-hole pair creation energy (4H-SiC) : $\epsilon_{e^-h^+} = 7.28 \text{ eV}$
- Elementary charge : $e = 1.60 \times 10^{-19} \text{ C}$

$$Q = \frac{E \cdot e}{\epsilon_{e^-h^+}} = (1.510 \pm 0.005) \times 10^{-4} \text{ nC}$$

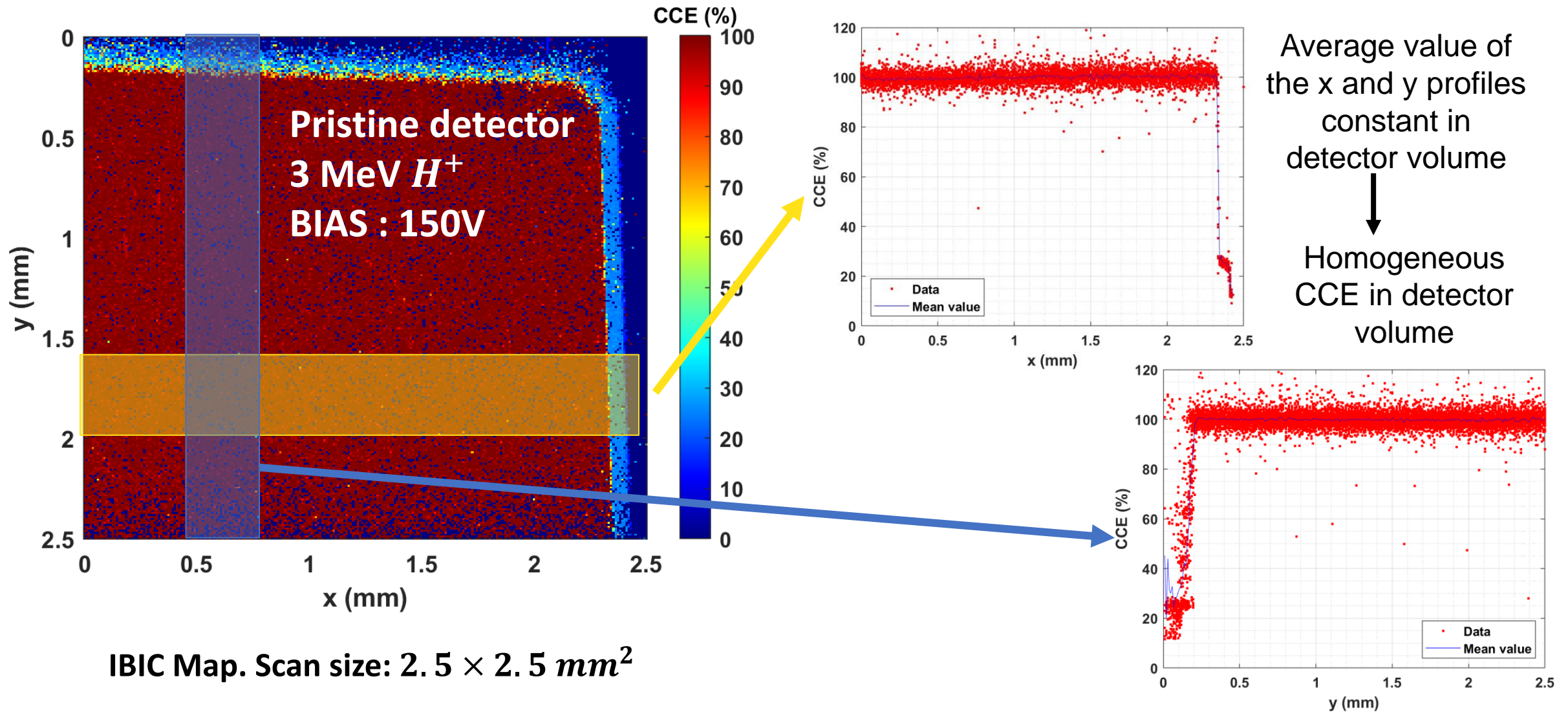
Experimental results :

- Integral = $(0.99 \pm 0.04) \text{ nWb}$
- Amplifier gain : (130 ± 10)
- Oscilloscope resistance : $R = 50 \Omega$

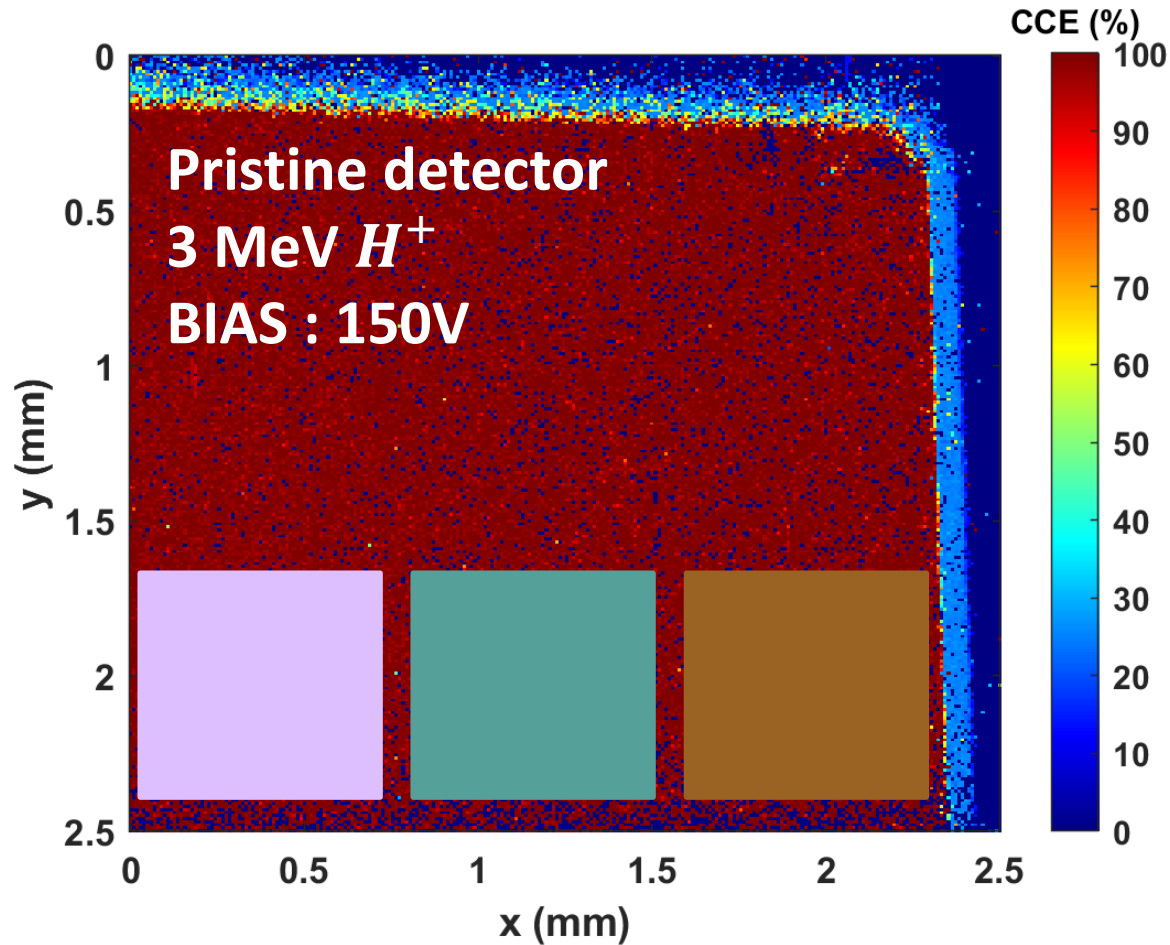
$$Q = \frac{I}{R \cdot G} = (1.52 \pm 0.18) \times 10^{-4} \text{ nC}$$

CCE = (101 ± 12)%

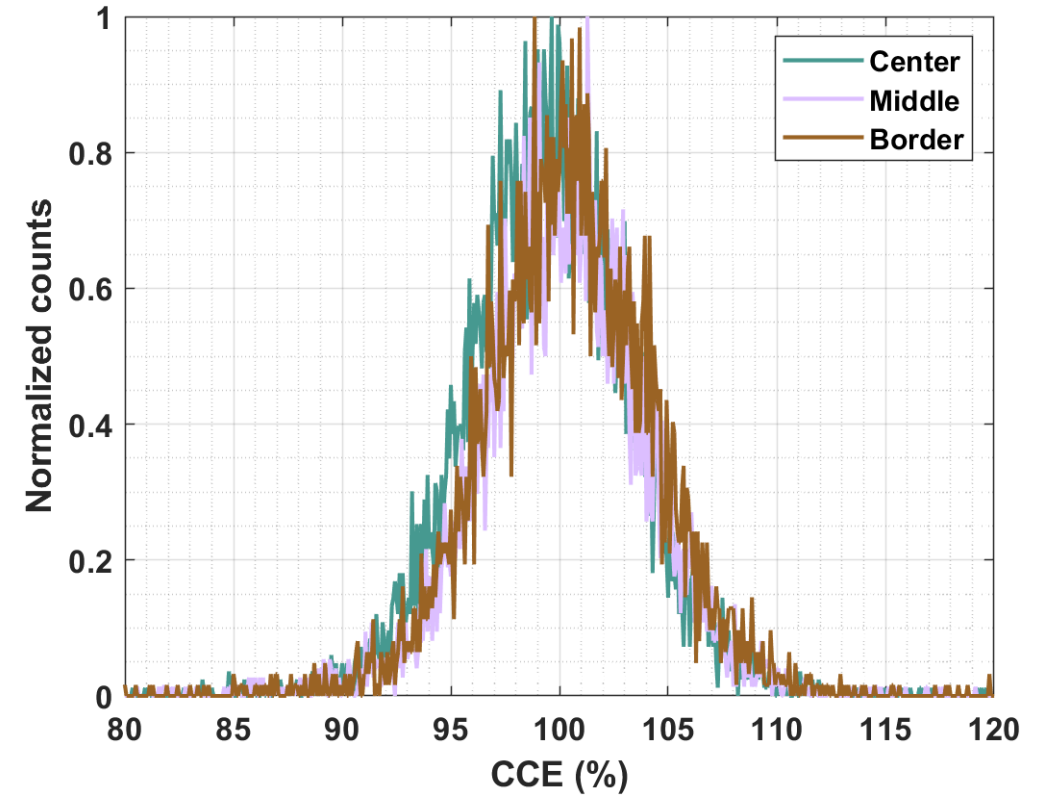
CCE homogeneity



CCE homogeneity



IBIC Map. Scan size: $2.5 \times 2.5 \text{ mm}^2$

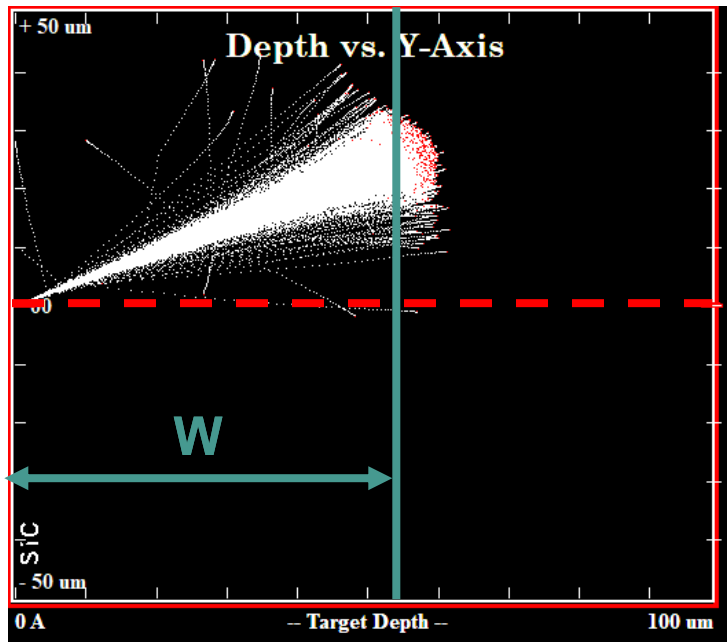


Identical position-
dependent local
spectra

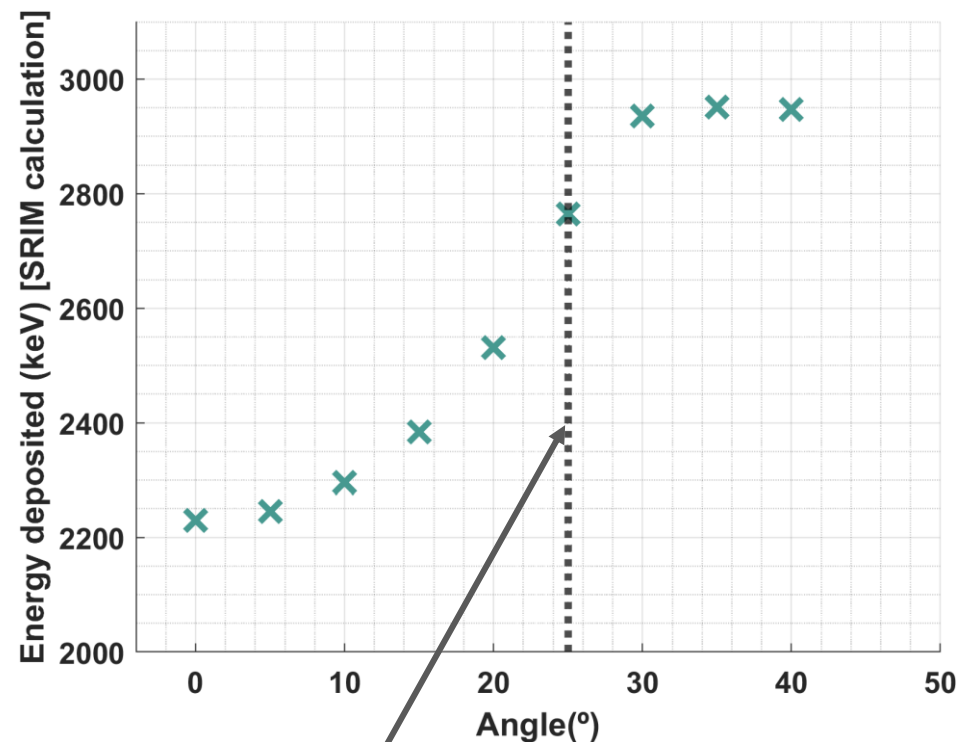
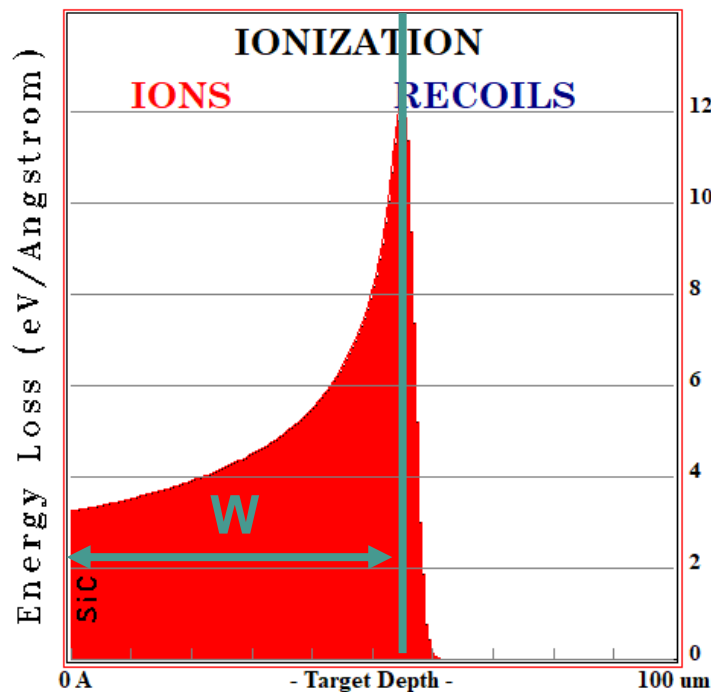


CCE is not radial
position
dependent

Critical angle

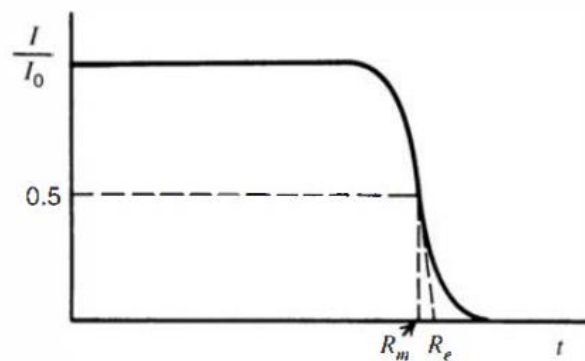


$$E_{dep}(W, \theta) = \int_0^W \frac{dE}{dx}(\theta) dx$$

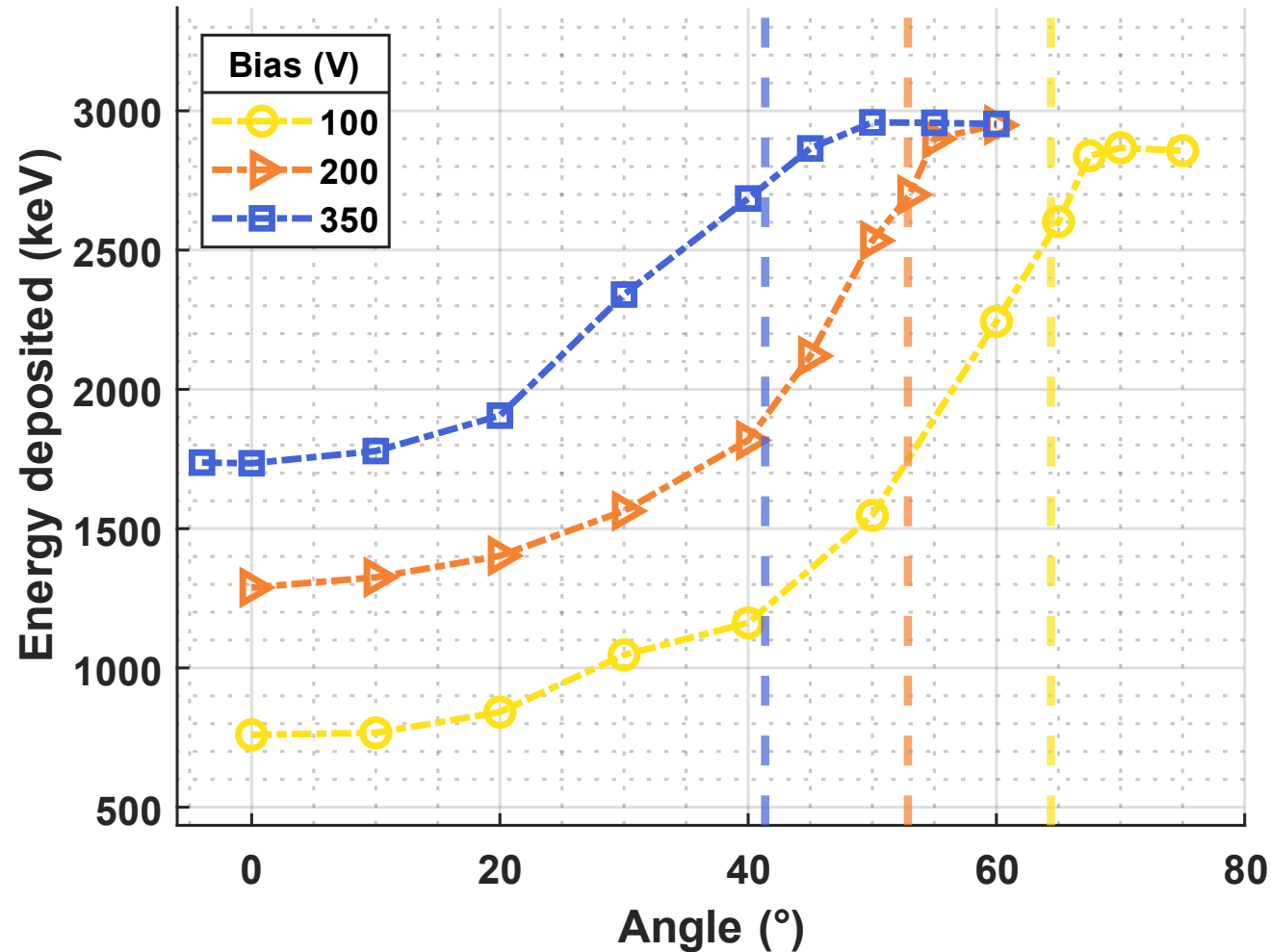


$$W[\mu\text{m}] = \text{Range}(E(\theta)) \times \cos(\theta)$$

$\theta \rightarrow$ critical angle



Critical angle

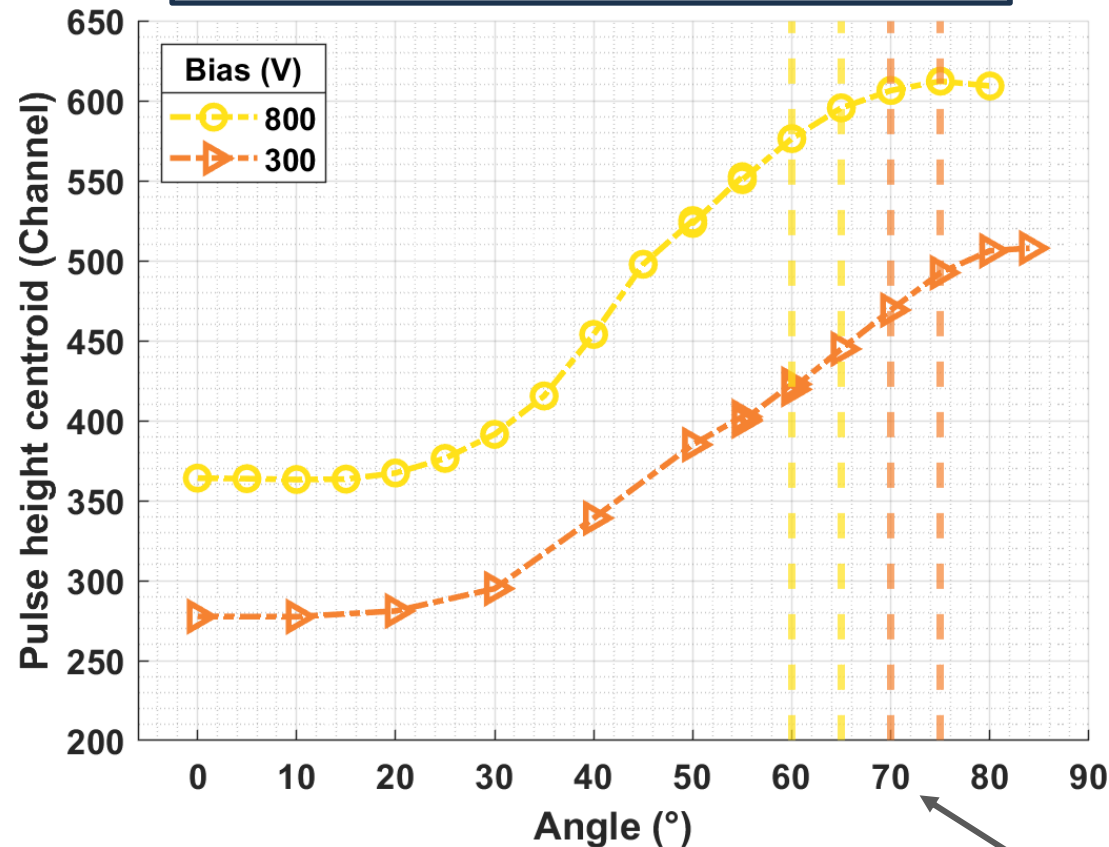


$$W[\mu\text{m}] = \text{Range}(E(\theta)) \times \cos(\theta)$$

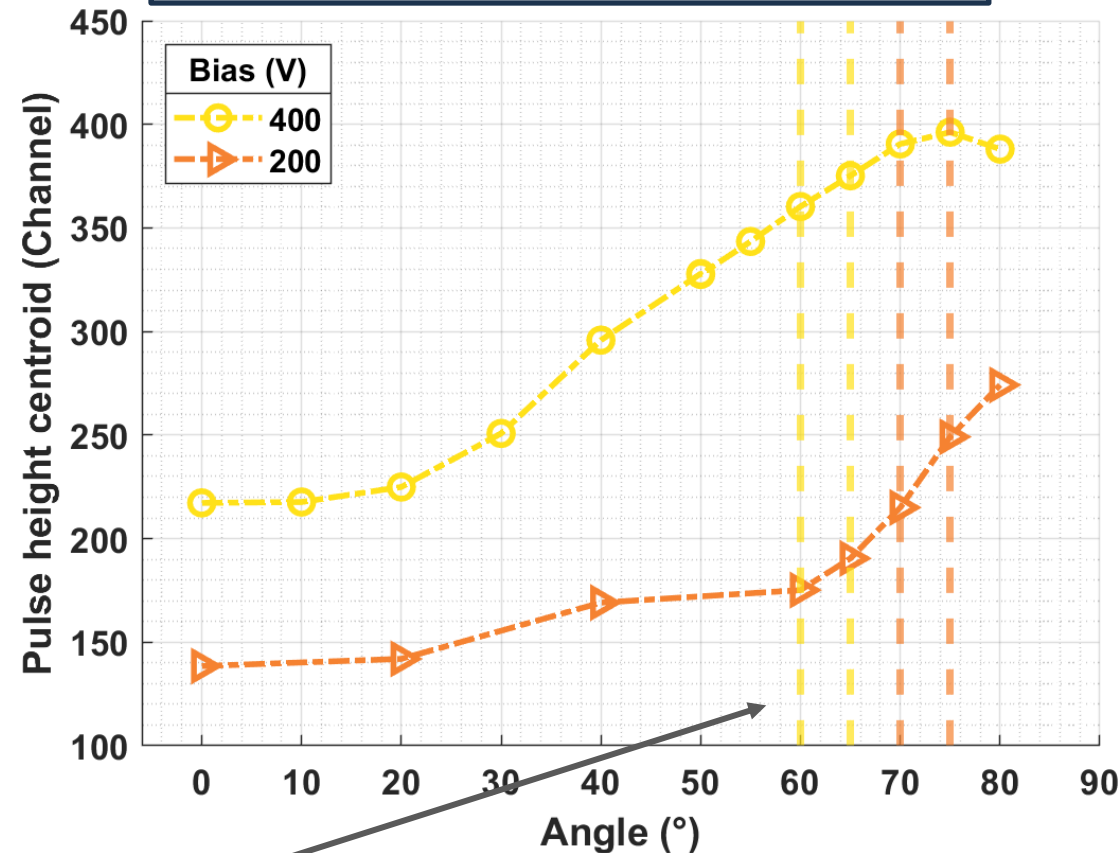
$\theta \rightarrow$ critical angle

Experimental results : Irradiated detectors

K6W1 ($4 \times 10^{14} n_{eq}/cm^2$)



F2W1 ($1 \times 10^{15} n_{eq}/cm^2$)

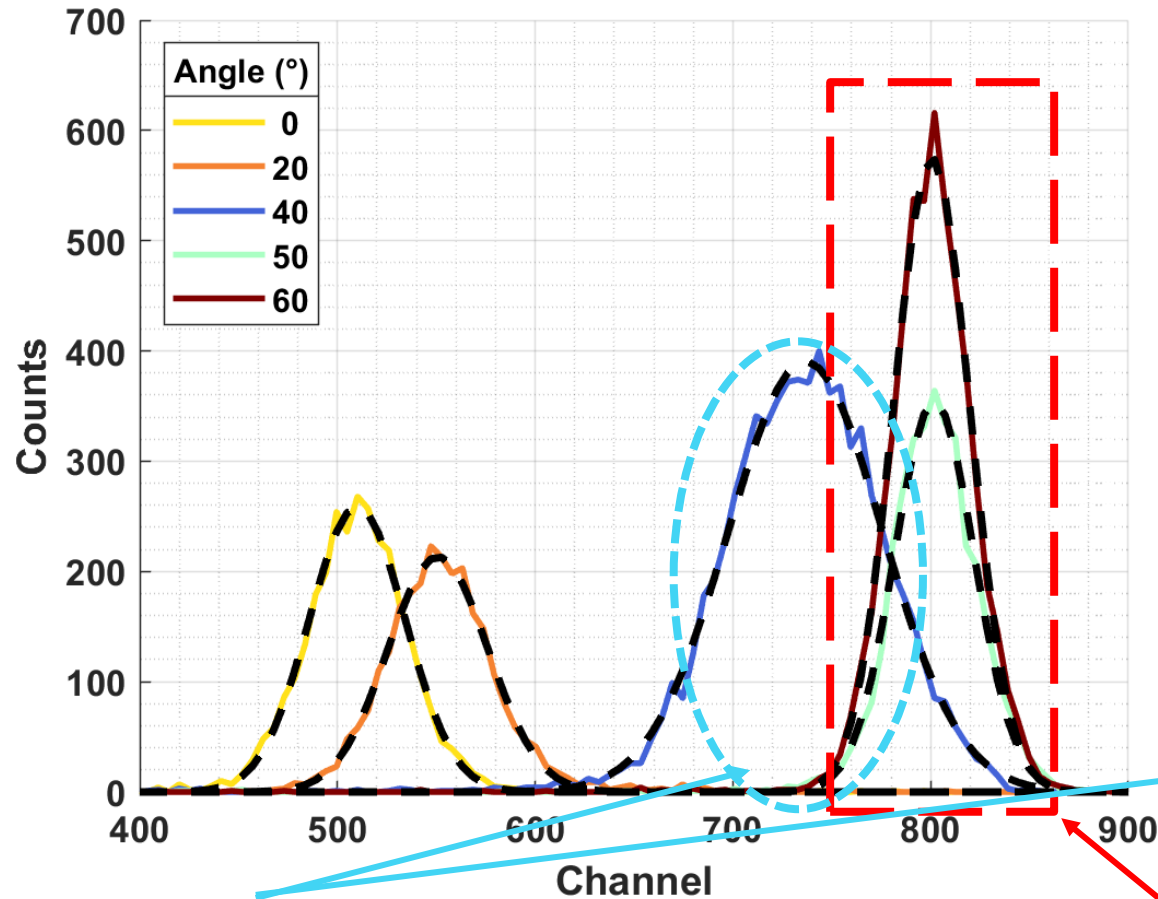


critical angles

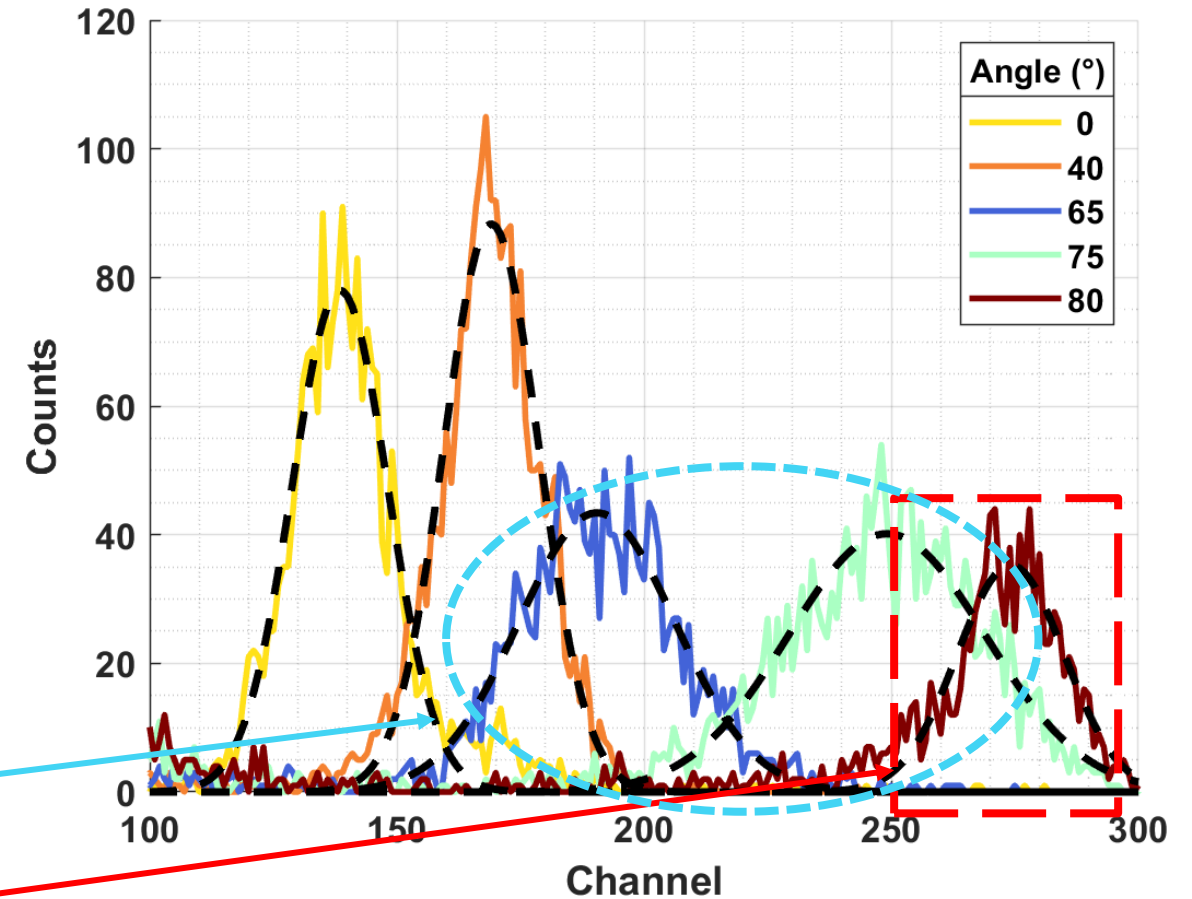
$$W[\mu\text{m}] = \text{Range} \times \cos(\theta)$$

Experimental results : Irradiated detector F2W1. Bias: 200 V

Protons 3 MeV. 1MW2 Bias = 350 V



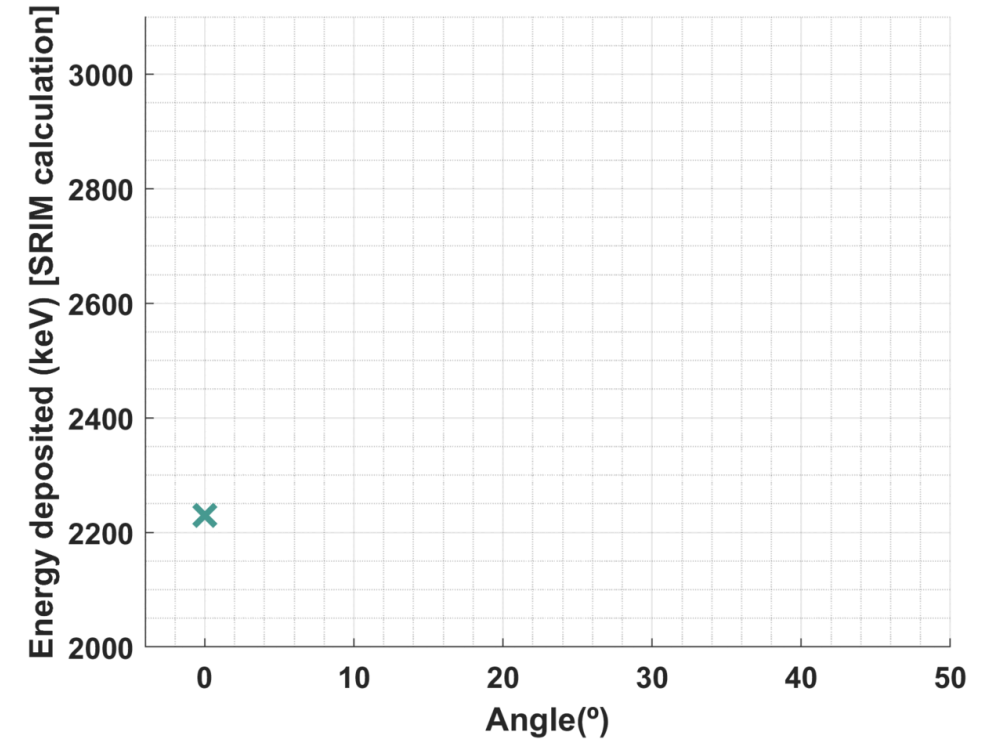
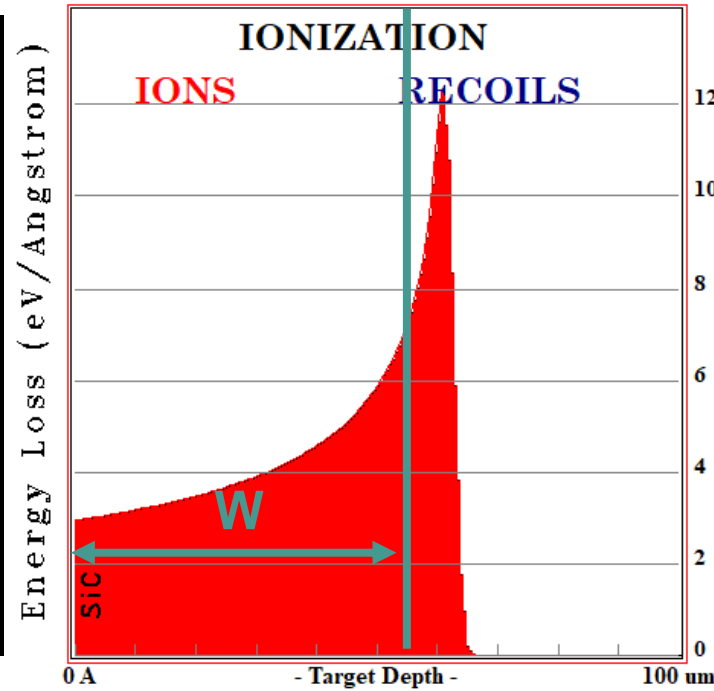
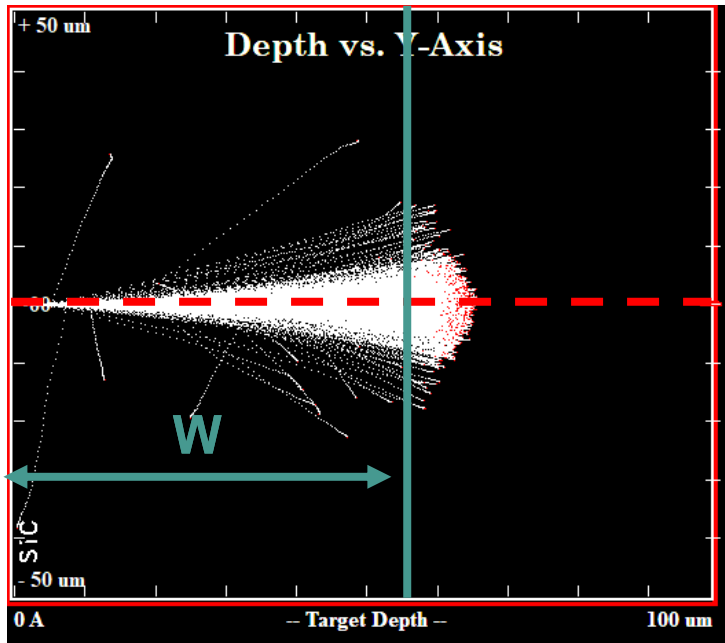
Protons 3 MeV. F2W1 Bias = 200 V



Critical angle → Angle before saturation angles

Saturation → Beam is completely within the sensitive volume

Methodology to calculate depletion zone



$$E_{dep}(W, \theta) = \int_0^W \frac{dE}{dx}(\theta) dx$$